Frequent origins of traumatic insemination involve convergent shifts in sperm and genital morphology

Jeremias N. Brand[1*], Gudrun Viktorin[1], R. Axel W. Wiberg[1], Christian Beisel[2], Luke J. Harmon[3] and Lukas Schärer[1]

[1] University of Basel, Department of Environmental Sciences, Zoological Institute, Vesalgasse 1, 4051 Basel, Switzerland

[2] Department of Biosystems Science and Engineering, ETH Zürich, Basel, Switzerland

[3] Department of Biological Sciences, University of Idaho, Moscow, USA

Short title:

Frequent origins of traumatic insemination

*Corresponding Author

University of Basel,

Department of Environmental Sciences, Zoological Institute,

Vesalgasse 1, 4051 Basel, Switzerland

Email: jeremias.br@gmail.com

Abbreviations

PC: principal component

pPCA: phylogenetically corrected principal component analysis

Abstract

Traumatic insemination is a mating behaviour during which the (sperm) donor uses a traumatic intromittent organ to inject an ejaculate through the epidermis of the (sperm) recipient, thereby frequently circumventing the female genitalia. It likely evolves due to sexual selection and sexual conflict, since it allows the donor to bypass pre- and postcopulatory choice and resistance mechanisms of the recipient. Several striking cases of traumatic insemination have been studied to date, but the frequency of its evolution, the intermediate stages via which it originates, and the morphological changes that such shifts involve remain poorly understood. Based on observations of reproductive traits in 145 species of the free-living flatworm genus *Macrostomum*—in combination with a robust phylogenomic phylogeny—we present comparative work on the evolution of traumatic insemination. We identify at least nine, but up to 13, independent origins of traumatic insemination, which involve convergent shifts in both sperm design and male and female genital morphology. We further find that traumatic insemination may originate via internal wounding. Finally, we highlight the large diversity of reproductive traits across the genus and show evidence for male-female coevolution. Our findings indicate that sexual selection and sexual conflict repeatably favour the evolution of behaviours—like traumatic insemination—that allow donors to bypass control mechanisms of recipients, leading to predictable shifts in both male and female reproductive traits.

Keywords: traumatic mating, hypodermic insemination, copulatory wounding, phylogenetics, evolution, female genitalia, correlated evolution, parallel evolution, sexually antagonistic coevolution

Introduction

The sexes frequently show a difference in mating propensity because male fertility (i.e. fertilized egg production) is often limited by the number of matings a male can achieve, while female fertility is often limited by the amount of resources a female can invest into eggs and offspring [1–3]. The resulting conflict over mating rate has far-reaching consequences, often resulting in "Darwinian sex roles" with choosy females and eager males [4]. Choice may be beneficial for females, since it allows them to preferentially reproduce with males based on genetic compatibility, genetic quality [5] and/or direct benefits (e.g. nuptial gifts [6]). Indeed, evidence for female choice is abundant and there are many species where females mate multiply, suggesting that polyandry may indeed result in such benefits [7]. However, females may also simply mate multiply as a result of male harassment, and while multiple mating could be costly to females, resisting male harassment might be even costlier [7, 8]. Costly harassment is expected to arise frequently, since female choice necessarily goes against the rejected males' interests [9], potentially leading to sexually antagonistic coevolution between male persistence and female resistance traits [8, 10, 11].

In polyandrous species, sexual selection and sexual conflict will continue after copulation through intricate interactions of the female genital tract with the male intromittent organs and the received ejaculate [12–14]. Female genitalia might exert postcopulatory control mechanisms through differential sperm storage, sperm ejection or sperm digestion, thus applying a selective filter on male genital and ejaculate traits. In analogy to the precopulatory conflict, it is then possible for traits in males to arise that attempt to bypass or influence the female choice and resistance mechanisms, again resulting in sexually antagonistic coevolution.

Sexually antagonistic coevolution can drive the emergence of male traits that inflict considerable harm on females [11, 15, 16]. A striking example that implicates such harm is traumatic insemination, which occurs in some internally fertilising species and involves the infliction of a wound to the female's integument through which the male then transfers its ejaculate [17]. Since traumatic insemination frequently occurs in both gonochoristic (separate-sexed) and hermaphroditic species

73 [17], we in the following use the more general terms (sperm) donor and (sperm) recipient to refer to
74 the two sexual roles, with no loss of generality [18].
75 Although traumatic insemination often results in costs to the recipients [15, 17, 19–22], it has evolved
76 repeatedly across various animal groups [17]. While natural selection might play a role in its evolution
77 in some taxa—especially the endoparasitic Strepsiptera [23, 24]—it likely often evolves because it
78 allows the donor to bypass pre- and postcopulatory choice and resistance mechanisms of the recipient.
79 Specifically, traumatic insemination can enable donors to force copulation and thus minimise the
80 control that the recipient could otherwise exert over mating [15]. Traumatic insemination usually also
81 allows the donor to bypass the recipient's genitalia, by depositing sperm either closer to the site of
82 fertilisation [24, 25] or even directly within the relevant tissue [15, 26], thus likely reducing the
83 recipient's ability to control the fate of the received ejaculate [12, 17]. In this view, traumatic
84 insemination allows the donor to bypass the influence of the recipient's sexually antagonistic choice
85 and resistance mechanisms, temporarily gaining an advantage in the coevolutionary chase.
86 However, since conflicts persist under traumatic insemination, we expect selection to then act on
87 traits that allow the recipient to regain control over mating and/or the fate of the received ejaculate.
88 For example, some species of bed bugs have evolved what could be considered a secondary vagina,
89 a structure that has been shown to reduce the costs incurred due to traumatic insemination [19, 27].
90 But even without the emergence of new organs, the recipients could evolve behavioural or
91 physiological responses to avoid traumatic insemination (such as parrying strikes during penis
92 fencing in polyclad flatworms [28]) or to manipulate and control the hypodermically received
93 ejaculate (e.g. similar to sperm digestion in copulating species [29–31]).
94 Besides bypassing recipient choice and resistance mechanisms, traumatic insemination could also
95 evolve due to sperm competition, since in many internally fertilising species sperm of unrelated
96 donors compete within the female genital tract for fertilisation of the recipient's eggs [32]. In this
97 context, traumatic insemination might allow donors to bias sperm competition in their favour and
98 prevent competing donors from removing their previously donated sperm, potentially resulting in

99 paternity benefits [17]. Indeed, traumatic insemination seems to affect sperm competition in a family
100 of spiders, where sperm precedence is biased towards the first male in a species with traumatic
101 insemination, while it is biased towards the second male in its non-traumatically mating relatives [17,
102 23, 33]. In contrast, traumatic insemination is associated with last male precedence in one species of
103 bed bug [26], so the effects of it on sperm competition might depend on a species' morphology and
104 ecology.
105 Interestingly, since traumatic insemination likely affects not only how sperm interact, e.g. concerning
106 sperm mixing, sperm removal and sperm density, but also the degree to which they are accessible to
107 recipient control, it could influence the nature of both sperm competition and cryptic female choice.
108 Cryptic female choice, sperm removal, and sperm displacement can introduce skews in the
109 distribution of sperm competing in the female storage organ, which may reduce the intensity of sperm
110 competition [34–38]. These same postcopulatory mechanisms can also favour sperm designs that
111 increase the chance of being retained in storage. This could include adaptations to better anchor or
112 position sperm, making them able to resist removal or displacement by either rival donors or the
113 recipient [39]. Traumatic insemination could lead to less removal and more mixing, resulting in a
114 more fair-raffle like sperm competition [40, 41], in which paternity success is more determined by
115 the relative number of sperm donated, leading to strong selection on sperm number. Since sperm
116 number is generally assumed to trade-off with sperm size [42–45], it is expected that traumatic
117 insemination is associated with smaller (and potentially also more numerous) sperm [40, 41].
118 Traumatic insemination might evolve more frequently in hermaphrodites due to sexual conflict over
119 mating roles [12, 18, 46–48]. In general, and in analogy to the situation outlined above for
120 gonochorists [1], a hermaphrodite that already carries enough received sperm to fertilise its own eggs
121 might gain little from additional matings as a recipient, while it might still gain additional
122 fertilisations by acting as a donor [12]. It is thus likely that, on average, individual hermaphrodites
123 show a preference for sperm donation [12, 18, 46–48] and this prediction is supported in several
124 laboratory studies [47, 49, 50]. Traumatic insemination then potentially allows unilateral enforcement

125 of donation while avoiding receipt. Additionally, harmful traits are expected to evolve more readily
126 in simultaneous hermaphrodites because fitness costs incurred by a recipient may be partially
127 compensated by fitness benefits from the same individual acting as a donor. A hermaphrodite may
128 thus also engage in matings that involve harmful effects, as long as the net fitness benefits of mating
129 are positive [46, 51]. Therefore, hermaphrodites could engage in traumatic insemination even if this
130 results in considerable harm to the recipient.

131 Indeed, traumatic insemination appears to arise more commonly in simultaneous hermaphrodites
132 compared to gonochorists, since they comprise 11 out of the 23 well-supported independent origins
133 listed in [17], which is a lot considering that hermaphrodites make up ~6% of animals [52].
134 Hermaphroditic animals are thus ideal study organisms for investigations of traumatic insemination,
135 since—while it has been studied in some charismatic systems [15, 25, 28, 53–56]—we know little
136 about how frequently it evolves or via which intermediate states a copulating species can transition
137 to traumatic insemination [17, 20, 22].

138 Here we present comparative work on the evolution of traumatic insemination across the genus
139 *Macrostomum*, a species-rich taxon of hermaphroditic free-living flatworms. In *Macrostomum*,
140 traumatic insemination is called hypodermic insemination, since in several species the donor uses a
141 needle-like stylet (**Fig 1**) to inject sperm through the epidermis of the mating partner and sperm then
142 move through the body of the recipient to the site of fertilisation [41, 57, 58]. Injected sperm can
143 often be observed inside the parenchymal tissues of these highly transparent animals [41, 57–59],
144 making it feasible to screen a large number of species for the convergent evolution of hypodermic
145 insemination. And while we here present evidence that not all traumatically mating *Macrostomum*
146 species may inject sperm through the external epidermis, we nevertheless use the term hypodermic
147 insemination for consistency with the earlier literature.

148 The genus consists of two phylogenetically well-separated clades, with one clade currently thought
149 to only mate through hypodermic insemination ("hypodermic clade", referred to as Clade 1 in [41])
150 and a second clade primarily containing reciprocally mating species ("reciprocal clade", referred to

151 as Clade 2 in [41]). Within the reciprocal clade, hypodermic insemination has previously been shown
152 to have convergently evolved in *M. hystrix* [41]. Reciprocally copulating *Macrostomum* species
153 engage in a copulatory handshake, where two individuals insert their often relatively blunt stylet (Fig
154 1) via their partner's female genital opening into the female sperm storage organ, the female antrum
155 (further only called antrum), so that both can donate and receive sperm in the same mating [60]. Many
156 reciprocally copulating species then perform a postcopulatory behaviour, where worms place their
157 mouth over their own female genital opening and suck [41, 61], presumably in an attempt to remove
158 components of the received ejaculate from the antrum (called the suck behaviour, [39, 60]). This
159 removal of ejaculate could target manipulative seminal fluids, since the ejaculate of the main
160 *Macrostomum* model species, *M. lignano*, contains substances that influence the mating partners
161 behaviour, including the propensity to perform the suck behaviour [62, 63]. The suck behaviour could
162 also be aimed at reducing the number of stored sperm (e.g. to lower the risk of polyspermy), constitute
163 a form of cryptic female choice (e.g. to favour donors of higher quality), and/or represent a resistance
164 trait in sexual conflict over mating roles (i.e. to undo unwanted sperm receipt) [41].
165 If the suck behaviour is a recipient resistance trait, we might expect the evolution of donor persistence
166 traits, potentially leading to antagonistic coevolution [8]. Indeed, the sperm of reciprocally copulating
167 species generally have a thin anterior feeler and two stiff lateral bristles that could represent such
168 persistence traits (**Fig 1**), serving to anchor the sperm in the antrum to prevent removal during the
169 suck behaviour [39, 41]. In contrast, sperm of species with hypodermic insemination (i.e. the
170 hypodermic clade and *M. hystrix*) lack lateral bristles and have a simplified morphology, presumably
171 because they no longer need to resist the suck behaviour [39, 41] which has so far never been observed
172 in species with hypodermic insemination. These sperm may instead be adapted to efficiently move
173 through the partner's tissues (**Fig 1**), and one such adaptation could include a size reduction, as
174 outlined above. Moreover, while species with reciprocal copulation have an antrum with a thickened
175 epithelium, the species with hypodermic insemination have a simple antrum, presumably because it
176 no longer interacts with the donor's stylet and sperm, and instead is used for egg-laying only [41].

177 Based on these findings, the observed adaptations to reciprocal copulation and hypodermic
178 insemination have been described as the reciprocal and hypodermic mating syndrome, respectively,
179 since they each constitute specific combinations of morphological (sperm, stylet and antrum) and
180 behavioural traits [41].

181 If hypodermic insemination evolved as a resolution of sexual conflict over the mating roles, then we
182 would expect it to occur frequently, but it is currently unclear whether hypodermic insemination has
183 convergently arisen more than once within the reciprocal clade. It is also unclear if the transitions are
184 reversible or if the emergence of hypodermic insemination alters the coevolutionary dynamics
185 between donor and recipient, so that they cannot readily revert back to reciprocal copulation. Little
186 molecular data is currently available for most species in the genus *Macrostomum* and the description
187 of important structures, such as the sperm morphology and aspects of the mating behaviours, are often
188 neglected in the taxonomic literature.

189 Here we collected molecular and morphological information on 145 *Macrostomum* species to identify
190 additional independent origins of hypodermic insemination, to highlight species that represent
191 possible transitional states in the evolution of hypodermic insemination, and to quantitatively assess
192 convergent changes in both sperm design and in male and female genital morphology that accompany
193 its evolution. Using ancestral state reconstruction, we further ask whether species can revert back to
194 reciprocal copulation once hypodermic insemination has arisen. Moreover, if hypodermic
195 insemination evolves in the context of sexually antagonistic coevolution, then signatures of male-
196 female coevolution in the form of a diversity of resistance and persistence traits should be evident
197 across the genus. Indeed it is predicted that donors might carry multiple persistence traits even if
198 recipients resistance renders them ineffective [64]. We thus test for covariation between male and
199 female genital morphology and survey the genus for novel resistance and persistence traits.

200 # Results

201 ## Species collected and phylogenetics

202 We included 145 *Macrostomum* species in our analysis, and established a phylogeny inferred from a
203 combination of newly generated transcriptome data (98 species, see Material and Methods) and a
204 partial *28S rRNA* gene sequence (permitting to add 47 additional species). Except for 14 species, we
205 collected and systematically documented all species ourselves. Based on an integrative approach—
206 using detailed documentation of *in vivo* morphology and *28S rRNA* sequences—we identified 51
207 species as previously described and a striking 94 species as likely new to science (see Material and
208 Methods for details on species delimitation; **Tab 1** for a summary of all collected species; **Tab S1** for
209 the sample sizes of morphological measures across species; and also SI Taxonomy). Since our focus
210 here was not on taxonomy, we delimited new species as operational taxonomic units. We deposited
211 extensive image, video [65], geographic and molecular data for all specimens collected and their
212 operational species assignment (see **Tab S2**), facilitating their future description (see
213 http://macrostomorpha.info and [65]).
214 We inferred phylogenies based on two protein alignments generated from transcriptome data (see
215 Material and Methods), one with many genes while having lower occupancy (L alignment with 8218
216 genes) and one with high occupancy but fewer genes (H alignment with 385 genes, **Tab 2**). For both
217 alignments, we calculated phylogenies using maximum likelihood with IQ-TREE [66] (referred to as
218 L-IQ-TREE and H-IQ-TREE) and summary methods with ASTRAL III [67] (L-ASTRAL and H-
219 ASTRAL). We applied summary methods to account for incomplete lineage sorting and the gene tree
220 – species tree conflict it can cause. Second, to include species for which we lacked transcriptomes,
221 we added information from *28S rRNA* to the H alignment to construct a combined (C) maximum
222 likelihood phylogeny (C-IQ-TREE, see Material and Methods). Third, we performed two types of
223 Bayesian analyses on the H alignment, one that like the maximum-likelihood analysis operates on
224 partitioned amino acids [68] (H-ExaBayes) and a second performed on the unpartitioned DNA coding

225 sequence alignment to better account for rate heterogeneity across sites [69] (H-PhyloBayes, see
226 Material and Methods).

227 Across these phylogenies, all species represented by more than one transcriptome (i.e. 15 x 2, 3 x 3,
228 and 1 x 9 transcriptomes) were monophyletic, with the notable exception of *M. lignano* (**Fig S1**). One
229 of the *M. lignano* transcriptomes was from the DV1 inbred line from the type locality near Bibione,
230 Italy [70] and the other from an outbred population from the Sithonia Peninsula, Greece [61, 71].
231 *M. lignano* was monophyletic in the L-IQ-TREE, H-PhyloBayes, and both ASTRAL phylogenies,
232 but the Greek population was sister to *M. janickei* in the H-IQ-TREE and H-ExaBayes phylogenies,
233 although node support for this split was low for H-IQ-TREE (**Fig S1**), and removal of cDNA synthesis
234 primer sequences from the alignment rendered *M. lignano* monophyletic in H-IQ-TREE (see SI
235 Primer removal and Material and Methods). A closer investigation of the morphology of the Greek
236 vs. Italian population also revealed that the former had a considerably larger stylet (96.7 vs. 60.7 µm)
237 and longer sperm (76.5 vs. 62.7 µm). We still consider *M. lignano* a proper species, but a closer
238 comparison of the Greek and Italian populations would be interesting.

239 Next, we discuss other agreements and discrepancies between the different inferred phylogenies. The
240 grouping of the major clades was mostly consistent across all phylogenetic approaches (**Fig 2** and
241 **Fig S1**). All phylogenies recovered six large species groups (further called the hypodermic, spirale,
242 lignano, finlandense, tuba, and tanganyika clade), two smaller species groups (the minutum and
243 hamatum clade), and two consistent species pairs (*M*. sp. 45 + 46 and *M*. sp. 4 + 89). However, the
244 backbone, and the positions of some species with long branches (*M*. sp. 37, *M*. sp. 39, *M*. sp. 90 and
245 *M. curvituba)*, differed depending on the alignment and method used. Despite these discrepancies,
246 the Robinson-Foulds distances [72] between the phylogenies were low (**Tab S3**), indicating good
247 agreement between methods.

248 In all phylogenies, the hypodermic clade was deeply split from the reciprocal clade, but with large
249 phylogenetic distances also appearing within the hypodermic clade (see also below). Also consistent
250 was the grouping of the tanganyika, tuba and finlandense clades (**Fig 2** and **Fig S1**). The hamatum

251 and minutum clades, together with *M.* sp. 4 + 89, were always the closest relatives to the former three
252 clades. However, the exact relatedness patterns were uncertain. In the L-IQ-TREE, H-IQ-TREE and
253 H-ExaBayes phylogenies, *M*. sp. 4 + 89 were the closest relatives to these three clades, followed by
254 the hamatum and minutum clades. In contrast, in the ASTRAL and the H-PhyloBayes phylogenies,
255 the hamatum clade was more closely related to the minutum clade (with the latter nested within the
256 former in case of H-PhyloBayes) and both were sister to the grouping of tanganyika, tuba and
257 finlandense. Moreover, the exact branching order at the base of the reciprocal clade was not clearly
258 resolved. The spirale clade split off first in the H-IQ-TREE and H-PhyloBayes phylogenies, while
259 the lignano clade split off first in the other phylogenies. Consistent with the conflict between methods,
260 the quartet support from the ASTRAL analysis indicated gene tree – species tree conflict at most
261 nodes in the phylogeny's backbone (**Fig S2**). These internal nodes were separated by short branches
262 suggestive of rapid speciation events, such as during adaptive radiation [73], where substantial
263 incomplete lineage sorting is expected. This pattern is also consistent with ancient hybridisation,
264 which is a distinct possibility, since there is evidence for hybridisation within the genus under
265 laboratory conditions [74].

266 The topology of C-IQ-TREE was identical to H-IQ-TREE when we removed all the species added
267 based on *28S rRNA* (**Fig 3**) and thus adding these species did not negatively influence the overall
268 topology of the tree. Node support in C-IQ-TREE was somewhat lower, as could be expected given
269 the placement of the additional species based solely on *28S rRNA* sequences. Nevertheless, the added
270 inferential power obtained from a ~50% increase in species representation is highly worthwhile, and
271 we therefore focus on results based on this combined phylogeny in the main text.

272 As already mentioned above, many species in the hypodermic clade were highly molecularly
273 diverged, even though they are difficult to distinguish morphologically. Most of these species had
274 stylets that consisted of a short proximal funnel that tapered to a curved and drawn-out asymmetrical
275 needle-like thickening (**Fig 3**A, top). It was possible to distinguish some species based on general
276 habitus. These differences are reflected by the four deeply split clades containing, *M. rubrocinctum*,

277 *M. hystricinum*, *M. gabriellae*, and *M. pusillum*, respectively (although the latter two clades were also
278 quite similar in habitus). We have indicated substantial morphological similarity by appending a letter
279 to the species name (e.g. *M. hystricinum a*, *c*, *d*). Investigations of species within the hypodermic
280 clade without support from molecular data thus require considerable caution. Moreover, given these
281 striking morphological similarities, it may often not be clear to which of these species the name-
282 bearing type specimens belong to [41], so the species names in this clade should be considered
283 tentative. Eventually, one may need to name these species afresh, applying more extensive molecular
284 species delimitation, and either suppress the original names of species without detailed enough
285 morphological descriptions and/or lacking adequate type material, or to define neotypes, including
286 molecular voucher specimens [75]. While such a detailed taxonomical revision of the genus
287 *Macrostomum* goes well beyond the scope of the current study, we feel that readers need to be aware
288 of these caveats (see also SI Taxonomy).

289 Morphological diversity

290 Before we report on our formal analysis of convergent evolution and coevolution, we highlight
291 several exciting morphologies, which considerably expand the known morphospace of *Macrostomum*
292 (**Fig 3**). As mentioned, the hypodermic clade shows little variation in terms of stylet and sperm
293 morphology. However, the stylet of *M*. sp. 93 differed clearly from that stereotypical form, by having
294 a small proximal funnel extending into a straight and obliquely-cut tube (**Fig 3**A). This shape is
295 similar to the stylets of several species in the reciprocal clade, namely *M. shenda*, *M*. sp. 34 and
296 *M*. sp. 64 (as well as *M. orthostylum*, for which we have no phylogenetic placement). Since we
297 observed hypodermic received sperm in both *M*. sp. 93 and *M*. sp. 64 (**Fig 3**), this shape appears
298 adapted for hypodermic insemination. And while we did not observe hypodermic received sperm in
299 *M. orthostylum* and *M*. sp. 34 (nor was such sperm reported for *M. shenda* by [76]), these species are
300 nevertheless likely to also mate through hypodermic insemination, not least since stylets with similar
301 shapes are also used for hypodermic insemination in related macrostomid flatworms [77].

302 In contrast to the largely canalized stylet and sperm of the hypodermic clade, we found remarkable
303 variation in these structures within the reciprocal clade (**Fig 3**). For example, we documented five
304 species in the spirale clade that had stylets with lateral protrusions close to the distal opening. The
305 protrusion is shaped like a rod or spike in *M. evelinae*, *M.* sp. 29 and *M.* sp. 42, while it consists of
306 two thin filaments in *M.* sp. 30 and *M.* sp. 43 (see also SI Taxonomy). These highly modified stylets
307 may have coevolved with the complex antra in these species, which have two separate chambers
308 connected via a ciliated muscular sphincter. The sperm of these species is also remarkable because
309 they carry only a single bristle instead of the typical two. The sperm of *M*. sp. 30 carry only a single
310 curved bristle, while the bristle of *M*. *evelinae*, *M*. sp. 29, and *M*. sp. 42 is additionally modified,
311 being thicker and appearing flexible, frequently curving back towards the sperm body. A second
312 bristle might also be absent in the closely related *M*. sp. 13 (indicated with a shaded second bristle in
313 **Fig 3**), but the available material currently does not allow an unambiguous assessment.

314 Sperm are also highly variable across the entire reciprocal clade. Particularly striking are the sperm
315 modifications of *M*. sp. 82, which give the anterior part of the sperm a translucent appearance under
316 phase contrast (discussed in more detail below). We also document extraordinarily long sperm in
317 several species in the tanganyika clade. While it is not entirely clear which part of the sperm is
318 modified here, it appears that they have very long sperm feelers, with the bristles thus being located
319 unusually far posterior. Finally, we observed numerous species that either had reduced (length <3.2
320 µm) or no sperm bristles. Such reduction and losses repeatedly occur across the whole reciprocal
321 clade and appear to coincide with changes in the stylet and antrum morphology (see our formal tests
322 below). Finally, a striking modification of sperm design occurs in *M. distinguendum* (finlandense
323 clade), which appears to lack sperm bristles, but instead carries novel club-shaped lateral appendages,
324 which in light microscopic images bear no resemblance to the usual sperm bristles.

325 The antrum morphology was also highly variable within the reciprocal clade, with several species
326 having complex female antra with multiple chambers. Particularly striking are the two female genital
327 openings present in four quite distantly related taxa (see SI Taxonomy). A second opening is present

328 in *M. spiriger*, *M. gieysztori* (and its three close relatives, *M.* sp. 16, *M.* sp. 17 and *M.* sp. 18),
329 *M. paradoxum*, and *M.* sp. 82, suggesting multiple independent origins across the genus (see SI
330 Female opening). The observed variation in male and female genital morphology, and sperm design
331 could be important for sexual selection, as we outline in the discussion.

332 Frequent origins of hypodermic insemination

333 We inferred the number of convergent transitions to hypodermic insemination using ancestral state
334 reconstruction (ASR) of three reproductive traits: received sperm location, sperm bristle state, and
335 antrum state (see SI Morphology and Tab 3). Because received sperm location involves the direct
336 observation of sperm within the recipient's tissue, it provides direct evidence for hypodermic
337 insemination. However, observation of injected sperm in field-collected specimens can be
338 challenging, especially in species with low investment into sperm production, thus lowering the
339 sample size. Since tests of correlated evolution revealed strong associations of hypodermic sperm
340 with absent/reduced sperm bristles and a thin antrum (see the next section), we also performed ASR
341 using these states as proxies for hypodermic insemination. Finally, we performed ASR on the inferred
342 mating syndrome, which represents a synthesis of all available information (see Material and Methods
343 and Tab 3). We performed ASR, with all traits scored as binary and, where appropriate, also as trinary,
344 to test if hypodermic insemination could evolve via an intermediate state (see Material and Methods).
345 All reconstructions indicated frequent origins of hypodermic insemination (Tab 4 and Fig S3). In all
346 analyses with trinary states, an ordered transition model without gains once traits have been lost
347 (ORD-Dollo) was preferred, and in all analyses with binary states, a model without gains (Dollo) was
348 preferred. However, other models, including some permitting gains, also received at least some
349 support (Tab 4). ASR of trinary states inferred frequent transitions to the intermediate state, which
350 were driven by the ordered model's requirements to transition through it. These transitions were often
351 placed along internal branches of the phylogeny, primarily within the finlandense clade, which
352 contains several species with reduced or absent states and, nested within them, two species with

353 present states (*M*. sp. 12 and *M*. sp. 44, with received sperm in the antrum, long bristles, and assigned
354 to the reciprocal mating syndrome; Fig S3 A, C, F).
355 We estimated a lower bound for the number of transitions by requiring an origin of the derived state
356 to be separated by other such origins via nodes with a >95% posterior probability of having the
357 ancestral state. Applying this rule to traits scored as binary, we find nine transitions to hypodermic
358 received sperm, 17 losses/reductions of sperm bristles, 13 simplifications of the antrum, and 13
359 transitions to the hypodermic or intermediate mating syndrome (see red stars and numbers in Fig S3).
360 Moreover, these lower-bound estimates were slightly lower for trinary states. Finally, we also
361 performed these analyses for the H-IQ-TREE and H-ExaBayes phylogenies, and found qualitatively
362 very similar results to those of the C-IQ-TREE phylogeny reported above, albeit, since they contain
363 fewer species, showing somewhat lower numbers of transitions (Tab S4).

364 Correlated evolution

365 We performed tests of correlated evolution to ask if the numerous convergent changes in received
366 sperm location, sperm bristle state and antrum state are evolutionarily dependent. We found strong
367 support for correlated evolution of received sperm location with both sperm bristle state and antrum
368 state (Fig 4A+B). This supports previous findings that hypodermic insemination is associated with
369 changes in sperm design and antrum simplification [41]. Therefore, when observations of received
370 sperm are missing, both sperm bristle state and antrum state are likely good proxies for the mating
371 syndrome. We expand on the earlier analyses by also providing evidence for the correlated evolution
372 between the sperm bristle state and antrum state (Fig 4C), which was implied in [41], but not formally
373 tested. We find substantially stronger support for correlated evolution than [41] across the board, with
374 Bayes factors that are 7.7 and 7 times larger for the correlated evolution of sperm bristle state or
375 antrum state with the inferred mating syndrome, respectively. Moreover, the analyses were robust,
376 with respect to the phylogeny and the priors used (see SI Correlated evolution).

377 ## Hypodermic insemination and convergence in morphospace

378 Next, we used phylogenetically corrected principal component analysis (pPCA) to investigate if these
379 convergent transitions to hypodermic insemination also coincide with changes in a greater variety of
380 reproductive traits (see SI Morphology). The first two principal components, PC1 and PC2, together
381 captured nearly half of the variation in the analysed reproductive traits (Fig 5), followed by additional
382 principal components with relatively small contributions (Tab S5). Specifically, PC1 captured a
383 change in stylet phenotype, with larger values indicating species with longer, more curved stylets,
384 that are distally more symmetric and less sharp (Fig 5). Larger values of PC1 also indicated both
385 longer sperm and bristles, and an increased probability for the sperm to carry a brush. Finally, high
386 values of PC1 indicated a thickened antrum with a more pronounced cellular valve, and a more
387 complex internal structure. In comparison, PC2 had a less clear interpretation, with high values
388 indicating larger species with larger proximal and distal stylet openings.
389 Species in the hypodermic clade (stippled outlines) had similar values in PC1 and mainly differed in
390 PC2. Interestingly, species from the reciprocal clade that we had assigned to the hypodermic mating
391 syndrome (solid and left yellow) grouped closely with the species in the hypodermic clade, indicating
392 striking convergence in morphospace concerning stylet, sperm and antrum morphology (see also Fig
393 S4). PC1 further separated species based on the received sperm location, with hypodermic received
394 sperm (right yellow) only found in species with low PC1 values, indicating that PC1 captures a
395 morphology necessary for hypodermic insemination. Almost all species with reduced (triangles) or
396 absent (circles) sperm bristles grouped closely together in PC1, with the notable exception of
397 *M*. sp. 68 and *M*. sp. 82 (black arrowheads), which cluster together with other species that we
398 assigned to the reciprocal mating syndrome. We observed sperm in the antrum of both species (i.e. in
399 2 of 7 specimens in *M*. sp. 68 and 16 of 21 specimens in *M*. sp. 82) and the antrum is similar in both,
400 with a long muscular duct that performs a 90° turn towards the anterior before it enters a second
401 chamber that is strongly muscular (Fig 6). Moreover, both species have a similar L-shaped stylet with

402 a blunt tip, which makes it unlikely that they mate through hypodermic insemination (see also
403 Discussion).

404 Pathways to hypodermic insemination

405 While 117 of the 145 studied species could be assigned to either the hypodermic or reciprocal mating
406 syndrome, some were not easily identified as performing either type of mating behaviour (Tab 3),
407 which may either have been due to lack of detailed observations, or more interestingly, due to
408 potentially transitional patterns that deviated from these syndromes. This included two species that
409 we categorised as intermediate because we observed sperm both in the antrum and embedded inside
410 the recipient's tissues (light green triangles in Fig 5). Both species (*M*. sp. 3 and *M*. sp. 101) have a
411 sharp stylet and sperm with reduced bristles, fitting with the hypodermic mating syndrome. But they
412 also have a thickened antrum wall, which indicates the reciprocal mating syndrome, and these species
413 indeed have intermediate values of PC1. Multiple observations of hypodermic sperm in *M*. sp. 3 show
414 them to be embedded deeply in the anterior wall of the antrum and more deeply in the tissue lateral
415 to the body axis, extending up to the ovaries, and in the tail plate (Fig 7). And while in *M.* sp. 101 we
416 did not observe sperm as deeply in the recipient's tissues, some were fully embedded in the cellular
417 valve and just anterior to it, and thus close to the developing eggs (Fig 8). One explanation for these
418 findings would be that during mating, the stylet of both species pierces the recipient's antrum wall
419 and sperm is traumatically injected into the body internally. Unfortunately, no copulations were
420 observed in mating observations of *M*. sp. 101, but this species has been seen performing the suck
421 behaviour, as expected if ejaculate is, at least partially, deposited in the antrum (pers. comm. P.
422 Singh). We lack mating observations for *M*. sp. 3 and further investigations of the mating behaviour
423 and the antrum histology of both species would be highly desirable.
424 Three additional species (*M*. sp. 14, *M*. sp. 51 and *M*. sp. 89) were also difficult to classify because,
425 although their morphology indicates hypodermic insemination, we clearly observed received sperm
426 in the antrum. *M*. sp. 51 and *M*. sp. 89 grouped with the hypodermically mating species in PC1 (red

427 arrowheads in Fig 5), while we did not include *M*. sp. 14 in this analysis due to missing data for sperm
428 bristle length. We found sperm within the antrum in only 1 of 4 specimens in *M*. sp. 51 and 1 of 12
429 specimens in *M*. sp. 89, and it is thus possible that sperm is hypodermically injected and may later
430 enter the antrum when an egg passes through the cellular valve into the antrum before egg laying. But
431 these species could also represent an intermediate state between the mating syndromes. We observed
432 sperm in the antrum in 3 of 5 specimens in *M*. sp. 14 and it therefore seems less likely that sperm
433 entering during the transition of the egg into the antrum is the cause of its presence here as well.
434 Instead, sperm is probably deposited in the antrum by the mating partner during copulation. However,
435 based on its general morphology, we predict that closer investigations of this species will reveal
436 hypodermic received sperm in a similar location as found in the other intermediate species (*M*. sp. 3
437 and *M*. sp. 101).
438 Finally, we were not able to assign *M*. sp. 10 to a mating syndrome, because—although we found
439 received sperm in the antrum and its sperm carry long bristles—it also has a sharp stylet and a simple
440 antrum. From our previous findings, we would expect this species to have a thickened antrum due to
441 its interaction with sperm and the mating partner's stylet. This discrepancy could possibly be
442 attributed to misclassification of the antrum morphology, since *M*. sp. 10 has very pronounced shell
443 glands, making it difficult to see the anterior part of the antrum, possibly obscuring a thickening or
444 cellular valve (see specimen IDs MTP LS 788 and MTP LS 801 for a possibly thin cellular valve).

445 Hypodermic insemination and sperm morphology

446 In addition to the changes in sperm design mentioned above, we tested whether hypodermic
447 insemination is associated with a change in sperm length using phylogenetic least squares (PGLS)
448 regression. We used received sperm location, sperm bristle state, antrum state, and the inferred mating
449 syndrome as predictors and the $\log_{10}$ transformed sperm length as the response variable. In all cases,
450 the states that indicate the reciprocal mating syndrome were associated with longer sperm, with the
451 largest effect for antrum state, followed by the inferred mating syndrome (Fig 9). This seems

452 reasonable, since the bristle type falsely classified *M*. sp. 68 and *M*. sp. 82 as hypodermically mating,
453 while the received sperm location and inferred mating syndrome analyses had lower samples size
454 than that with antrum state. The predictive value of the PGLS models was high, indicating that a large
455 proportion of the variation in sperm length is explained by the phylogeny and these indicators of the
456 reciprocal mating syndrome (Fig 9, Tab S6). Note that despite these strong associations, there is
457 considerable overlap in sperm length between the species exhibiting the different states, with some
458 species with the reciprocal mating syndrome having short sperm (Fig 9, Tab S6) and an overall 6.7-
459 fold variation in sperm length across all species (mean length ranging from 25.6 to 173.1 μm).

460 Coevolution of male and female genitalia

461 To investigate coevolution between male and female genital traits, we independently summarised five
462 male and four female genital traits using pPCA. Stylet PC1 was positively loaded with stylet length
463 and the width of the distal opening and negatively loaded with distal asymmetry. Therefore, high
464 values of Stylet PC1 represent a more elongate stylet with a wider and less sharp distal opening (Fig
465 10A, Tab S7). Antrum PC1 was positively loaded with all input variables, meaning that large values
466 represent more complex female genitalia (Fig 10B). A PGLS regression of Stylet PC1 on Antrum
467 PC1 across all species revealed a significant positive relationship (Fig 10C). This relationship closely
468 matches the loadings on PC1 in the pPCA analysis of all reproductive traits (see Fig 5) and could
469 therefore be mainly driven by the simplification of the antrum in hypodermically mating species.
470 Therefore, we repeated the analysis on the subset of species assigned to the reciprocal mating
471 syndrome. We again found a positive relationship between Stylet PC1 and Antrum PC1, indicative
472 of male-female coevolution of genital morphology among the reciprocally mating species (Fig 10C).

473 # Discussion

474 Across the genus *Macrostomum*, hypodermic insemination has evolved independently at least 9 times
475 when assessed based on the location of received sperm, and at least 13 times when our more inclusive
476 inferred mating syndrome is considered. The frequent origins of this type of traumatic insemination
477 is remarkable considering that according to Lange et al. [17] merely 12 and 11 such origins have to
478 date been documented in gonochorists and simultaneous hermaphrodites, respectively (including the
479 two cases previously documented in *Macrostomum*). Our detailed analysis of a single genus of free-
480 living flatworms thus approximately doubles the number of documented origins of hypodermic
481 insemination among hermaphrodites. Moreover, three additional origins of traumatic insemination
482 have also recently been documented in the Macrostomorpha [77], the parent group of the genus
483 *Macrostomum*, suggesting that the origin of traumatic insemination occurs commonly in the
484 Macrostomorpha, and maybe other groups of free-living flatworms.

485 The majority of the collected species are likely undescribed, and a large proportion of the diversity in
486 this genus is yet to be discovered. Since free-living flatworms remain understudied in many regions
487 of the world [78], we have likely not yet documented all convergent origins of hypodermic
488 insemination within *Macrostomum*. As a case and point, the deeply split placement of *M.* sp. 15 (from
489 South Africa) and *M.* sp. 118 (from Southern France) suggests the existence of an additional clade,
490 possibly hinting at large amounts of additional molecular diversity. While we have no observations
491 on the sperm morphology of *M.* sp. 15 or *M.* sp. 118, the stylet morphology of *M.* sp. 15 is suggestive
492 of hypodermic insemination, and closer investigations of this clade would be interesting since this
493 could facilitate inference about the ancestral state leading to the reciprocal clade.

494 Frequent convergent evolution of this extreme type of mating bolsters the interpretation that it
495 represents an adaptive resolution to sexual conflict over mating rate, mating role or both [12, 18, 28,
496 39, 41, 46]. Hypodermic insemination likely is an alternative strategy in an ongoing evolutionary
497 chase between donor and recipient, with donor persistence traits, such as complex sperm with bristles

498 and manipulative seminal fluids, and recipient resistance traits, such as the suck behaviour and
499 complex female genitalia, engaged in constant antagonistic coevolution [12, 17, 20, 46]. Moreover,
500 this coevolution does not only seem to drive the frequent origin of hypodermic insemination, but also
501 appears to result in the emergence of multiple morphological innovations, such as modifications of
502 stylet, sperm and antrum morphology (see also below).

503 Interestingly, we find no clear evidence for reversals back to reciprocal mating once hypodermic
504 insemination has arisen. However, while a Dollo model was preferred in all our ancestral state
505 reconstructions, this evidence was not completely decisive, as alternative models also received at
506 least some support. Reciprocal copulation clearly is the ancestral state of the reciprocal clade, but the
507 state of the most recent common ancestor of the genus is less clear, allowing for either a gain or a
508 loss (Fig S3). Similarly, in the finlandense clade we either have two independent losses with *M*. sp. 12
509 and *M*. sp. 44 retaining the ancestral state, or a single loss with a gain in these two sibling species
510 (Fig S3).

511 Since hypodermic insemination fundamentally alters the nature of the mating interaction, it might be
512 difficult for a species to revert to copulation. Specifically, once copulation no longer involves
513 inserting the stylet into the antrum, a reversal back to copulation would presumably require both
514 mating partners to again engage in a reciprocal behaviour. Also, a simplification of the antrum could
515 further hinder reversals, since reciprocally copulating species have traits that presumably reduce the
516 risk of injury (e.g. a thickened antrum epithelium). If these traits have been lost and are missing in
517 hypodermically mating species, then occasional reciprocal copulations could result in high fitness
518 costs for both partners.

519 In contrast, hypodermic insemination can presumably be performed unilaterally and might not require
520 the cooperation of both partners, making an evolutionary transition in that direction more likely.
521 Consequently, the origin of hypodermic insemination likely is a one-way process that canalises taxa
522 into this mating behaviour. However, across macroevolutionary time recipients may evolve
523 secondary female genitalia to avoid costs and regain control over the received ejaculate [17]. Why

524 this has not occurred in *Macrostomum* is unclear, but it might imply that costs of hypodermic
525 insemination are generally low (possibly due to the striking regeneration ability of these flatworms
526 [79]) or that the location of insemination is too variable for the evolution of a localised novel organ.

527 The analysis of correlated evolution clearly shows a strong association between both the sperm bristle
528 and antrum state with the received sperm location. While on first sight this might simply appear to
529 represent a confirmation of previous findings [41], albeit with more species and consequently a larger
530 Bayes factors, it actually represents a very important qualitative improvement of the evidence for
531 these associations. This is due to how tests of correlated evolution generally, and the Pagel test
532 implemented in the BayesTraits analysis specifically, are set up. Tests of correlated evolution evaluate
533 evidence for convergence, by testing whether a model, in which the evolution of the state of one trait
534 is dependent of the state of the other trait, is more likely than a model where such shifts occur
535 independently. While these tests supposedly correct for phylogenetic dependencies, they, somewhat
536 counterintuitively, can support the dependent model of evolution even with only a single
537 (unreplicated) origin of the trait states in question, provided that these origins map to appropriate
538 nodes in the phylogeny (as recently outlined: [80, 81]). However, descendants of a clade often share
539 multiple traits, many of which may not be functionally linked (as in the example given by [80] of the
540 joint presence of fur and middle ear bones in mammals). Naturally, one aim of such a correlation
541 analysis is to explore whether there might be a causal relationship between the traits in question.
542 Thus, while the previous findings with two independent origins of hypodermic insemination in
543 *Macrostomum* could be considered evidence for correlated evolution [41], that evidence is not as
544 decisive as the large Bayes factors may have suggested. By sampling many more convergent events,
545 we here could remedy the limitations of these earlier results, giving us substantially more confidence
546 that our findings indeed reveal a causal link between these traits and allowing us to evaluate the
547 consequences of shifts to hypodermic insemination in a more quantitative context.

548 In their earlier study [41] posited that specific combinations of adaptations were necessary for
549 efficient hypodermic insemination, consisting of a needle-like stylet and sperm adapted for movement

550 through tissue. As a consequence of hypodermic insemination, the antrum should then become
551 simpler, since it no longer interacts with the sperm and stylet of the partner, instead being only used
552 for egg-laying. While the data of [41] was suggestive, the issue was that the second hypodermic origin
553 consisted only of *M. hystrix*, which made quantitative analysis difficult. The principal component
554 analysis we performed here shows that species with hypodermic insemination indeed have similar
555 values of PC1, with such values corresponding tightly to the mating syndromes described by [41]
556 (but note that we here slightly adjusted the definitions of the syndromes, since we lacked behavioural
557 observations for most species). We show that hypodermic insemination is indeed associated with a
558 distinct syndrome of reproductive traits that have convergently evolved many times in this genus.
559 Therefore, these traits likely constitute predictable adaptations to this type of mating.
560 We observed several species with an unclear or intermediate mating syndrome, and these species
561 suggest a possible route to hypodermic insemination via the initial evolution of a traumatic stylet in
562 reciprocally mating species. A sharp stylet could provide anchorage during copulation, as potentially
563 occurs in *M. spirale* (pers. obs.) and *M. hamatum* (pers. comm. P. Singh), but it may also serve to
564 stimulate the partner during copulation, or aid in the destruction or removal of rival sperm already
565 present in the partner's antrum. Finally, internal wounding by the stylet may help to embed sperm in
566 the antrum wall and/or cellular valve to prevent their removal, either by rival mating partners or by
567 the recipient during the suck behaviour. However, the fact that we observe many *Macrostomum*
568 species with stylets with blunt distal thickenings (Fig 3) suggests that such internal wounding may
569 not always be advantageous for the donor and that these structures may have evolved to avoid harm
570 to the recipient [41]. Irrespective of the initial selective advantage that internal wounding may confer,
571 it could then evolve further to complete internal traumatic insemination, and eventually complete
572 avoidance of the female genitalia and hypodermic insemination via the epidermis.
573 Accidental sperm transfer due to copulatory wounding has generally been suggested as a possible
574 route from copulation to traumatic insemination (e.g. in traumatically mating bedbugs) [17, 20]. In
575 bedbugs, the attachment during mating is a two-step process, indicating that traumatic insemination

576 was evolutionarily preceded by traumatic penetration for attachment [17]. Similar transitions have
577 also been proposed for *Drosophila* species in the melanogaster group, where extragenital wounding
578 structures are typically used for anchorage during copulation. In traumatically inseminating
579 *Drosophila,* these structures are modified and pierce the mating partner's integument to inject sperm
580 into the genital tract [55, 82]. In this light our findings are remarkable, because previous examples
581 only compared species with and without traumatic insemination, whereas we potentially observe
582 species "in the act" of transitioning to traumatic insemination. These intermediate species should be
583 excellent targets for future studies of the costs and benefits of traumatic insemination, especially
584 because the two candidates represent independent evolutionary transitions.
585 The effects of traumatic insemination on sperm morphology are mostly unknown, and we are only
586 aware of the previous study on hypodermic insemination in *Macrostomum* [41]. We here present
587 quantitative evidence for a shift in sperm length under hypodermic insemination. The PGLS analysis
588 showed that, on average, the sperm of species with the hypodermic mating syndrome are significantly
589 shorter. There are several possible explanations for these findings. First, hypodermic insemination
590 avoids the recipient's genitalia, and these potentially allow both cryptic female choice (e.g. via the
591 suck behaviour), and sperm displacement or removal by competing donors. Hypodermic insemination
592 could therefore alter the mode of postcopulatory sexual selection and particularly sperm competition.
593 This is because postcopulatory sexual selection can introduce skews in sperm representation [35, 37,
594 38, 83], which likely results in lower sperm competition compared to a "fair-raffle" type sperm
595 competition, where sperm are expected to mix more freely [32, 43, 44]. Such skews seem less likely
596 to occur under hypodermic insemination. If sperm size trades-off with sperm number [42–44] then
597 more intense sperm competition under hypodermic insemination will likely favour the evolution of
598 smaller sperm [40, 41].
599 Second, sperm in *Macrostomum* is quite large compared to the size of the antrum, and it intimately
600 interacts with its epithelium, often being partially embedded in the cellular valve with the feeler [39,
601 41, 60, 84]. Sperm is also in close contact with rival sperm when animals mate multiply [85, 86].

602 Under such conditions of high sperm density, i.e. when sperm displacement is likely (e.g. [87–89]),
603 sperm are predicted to be bigger compared to species in which the sperm storage organ is substantially
604 larger than the sperm [45, 90]. While in species with hypodermic insemination the sperm will still
605 intimately interact with the partner's tissue, the "storage organ" could now potentially include the
606 whole body of the recipient and would then be considerably larger compared to the antrum. Third,
607 sperm size could decrease due to natural selection, if small sperm are better able to move through the
608 dense parenchymal tissue of the mating partner [41]. We know little about sperm movement within
609 the recipient's tissues, but it seems analogous to the movement one can observe within the antrum,
610 namely via undulation of the sperm body using cortical microtubules [91]. Presumably, smaller sperm
611 need less energy to overcome tissue resistance and thus might move more efficiently.
612 Note, that these three explanations are not mutually exclusive, and their relative importance might
613 depend on the physiology, morphology, and ecology of each species. Even though sperm morphology
614 is exceptionally diverse, little is known about its functional significance [92]. Because traumatic
615 insemination originates frequently, it offers an exciting opportunity to disentangle how natural and
616 sexual selection shape sperm morphology. Such investigations can contribute to an integrative view,
617 considering not only the sexual selection perspective, but also the direct functional constraints a
618 sperm's ecology imposes (e.g. survival in sperm storage vs. movement through tissue) [93].
619 To disentangle mechanisms shaping sperm length evolution, we should ideally investigate the sperm
620 morphology of other species with traumatic insemination and make use of natural variation in the
621 location of sperm injection. For example, in bedbugs, the elaboration of the sperm receiving organ
622 varies considerably from just being a slightly thickened epithelium to a complex spermalege [27, 94].
623 If movement efficiency is a crucial constraint, we might expect a negative correlation between sperm
624 length and tissue transit time. Also of interest are comparative investigations of sperm length in taxa
625 with species with traumatic insemination directly into the recipient's reproductive tract (e.g. the fly
626 *Drosophila parabipectinata* [55] or the spider *Harpactea sadistica* [33]), because here movement
627 through tissue is absent and presumably factors related to sexual selection dominate.

628 Besides changes in sperm length, we strengthen earlier findings that hypodermic insemination is
629 associated with the loss of sperm bristles [41]. Furthermore, we document hypodermic received sperm
630 in species with reduced bristles, indicating that hypodermic insemination likely precedes the complete
631 loss of bristles. The ancestral state reconstruction using three sperm bristle states found support for
632 an ordered evolutionary model, suggesting a transition via an intermediate state may be the rule. If
633 bristles only confer a selective advantage in reciprocally mating species, we could expect them to be
634 lost through drift once hypodermic insemination evolves, since these structures are no longer needed
635 to persist against the suck behaviour. Moreover, sperm bristles might also be selected against in
636 hypodermically mating species if they result in costs for the donor, such as a reduced rate of
637 spermatogenesis of complex sperm. Indeed, spermatogenesis of the complex sperm with bristles of
638 *M. lignano* takes about six days, which is two days longer than the development of the simpler sperm
639 in *M. pusillum* [95–97]. But note that this could also be due to sperm length differences between these
640 species, since longer sperm have been associated with longer development times [98, 99]. Moreover,
641 hypodermic sperm that carry bristles could also have reduced mobility [41].
642 The fact that there are hypodermically mating species with reduced bristles suggests that selection
643 might only be efficient at reducing bristle size until they no longer result in strong costs. Short bristles
644 might not hinder movement much, and once the bristles are reduced to such an extent that they do not
645 protrude much from the sperm, they could potentially be retained across longer evolutionary times.
646 The sperm of a member of the *M. pusillum* species-complex in the hypodermic clade contains
647 electron-dense bodies [100] that are similar to the bristle anchor structures identified in the
648 reciprocally mating *M. tuba* and *M. lignano* [91, 101]. If these structures are indeed remnants of
649 bristles, this would support the hypothesis (in agreement with our ancestral state reconstruction) that
650 bristles are symplesiomorphic in *Macrostomum*—with bristle loss as the derived condition—
651 suggesting that such greatly reduced bristles are not costly or detrimental to sperm function.
652 Moreover, sperm bristles have not been observed in three species of *Psammomacrostomum* (pers.
653 obs.), the sister taxon of *Macrostomum* in the Macrostomidae [77], nor in a presumably closely

654 associated genus (e.g. *Dunwichia* [102]). Sperm bristles thus appear to be a novel trait that is restricted
655 to the genus *Macrostomum* (and some closely associated and taxonomically problematic genera that
656 should be synonymised with *Macrostomum*; see SI Taxonomy). However, more detailed
657 investigations of sperm ultrastructure of species in the hypodermic clade and other Macrostomorpha
658 are needed to evaluate this hypothesis.
659 Our data further suggest that the correlation between reduced/absent bristles and the hypodermic
660 mating syndrome is not perfect, because we document two species without sperm bristles, that very
661 likely mate through reciprocal copulation (*M*. sp. 68 and *M*. sp. 82; black arrows in Fig 5). In both
662 species, we have observed sperm in the antrum that in both is very muscular and complex (**Fig 6**).
663 We speculate that sperm is deposited deeply inside the antrum, so that sperm bristles may no longer
664 serve an anchoring function in these species. Additionally, the sperm of *M*. sp. 82 has a peculiar feeler
665 (Fig 6), which could represent an adaptation to this complex antrum morphology. It is also not clear
666 if these species perform the suck behaviour, as this was not observed in mating observations of
667 *M*. sp. 82 (pers. comm. P. Singh), while we currently have no data at all on the mating behaviour of
668 *M*. sp. 68. The loss of sperm bristles in reciprocally mating species should caution us against a too
669 hasty conclusion that bristle loss is adaptive. Instead, bristles could be lost simply due to drift because
670 they no longer serve a function.
671 We also find clear evidence for male-female genital coevolution, both across all species and when
672 the analysis is restricted to species assigned to the reciprocal mating syndrome. This evidence is in
673 line with previous findings of such coevolution in hermaphrodites (e.g. [53, 103]) and contributes to
674 a growing body of evidence that male-female genital coevolution frequently occurs in both
675 hermaphrodites and gonochorists [104–107]. Genital coevolution is expected both under scenarios of
676 sexual selection and sexual conflict. Under the sexual selection perspective, we expect coevolution
677 due to cryptic female choice, where the recipient will choose based on genital traits of the donor
678 [108]. Donors are therefore selected to closely match their genital morphology to the selection criteria
679 of the recipient. Similarly, we expect coevolution to result from sexual conflict, since persistence and

680 resistance traits of the donor and recipient will coevolve due to sexually antagonistic selection [8].
681 The number and nature of the traits involved in this coevolution, as well as their respective selective
682 optima, might potentially differ between species, driving trait diversification and speciation [109,
683 110].
684 We see signatures of evolutionary diversification across the genus, with the emergence of several
685 novel and clade-specific traits. Five related species in the spirale clade carry lateral stylet protrusions,
686 which might serve to anchor the donor during copulation or allow sperm removal, and these species
687 have complex antra and an unusual sperm design with only a single bristle. Moreover, several species
688 in the tanganyika clade have long sperm, which could constitute a novel persistence trait serving a
689 similar function as is hypothesised for the sperm bristles. It appears possible that these long structures,
690 which are probably greatly elongated sperm feelers, can embed themselves in the recipient's antrum.
691 They may thereby anchor the sperm and help to prevent removal, making bristles less important to
692 resist the suck behaviour. Indeed, several of these species have quite short bristles (including the
693 above-mentioned *M.* sp. 68 that lacks bristles entirely), in spite of showing the reciprocal mating
694 syndrome, thus supporting this interpretation. Other novel traits include the peculiar sperm feeler of
695 *M*. sp. 82, the novel sperm appendages in *M. distinguendum*, and the frequent emergence of a sperm
696 velum, the function of which is currently completely unknown.
697 While coevolution can drive trait diversification, it is also interesting to consider cases of
698 convergence. Repeated origins of a trait indicate that it is a readily available target of selection.
699 Besides hypodermic insemination, another example of convergent evolution in *Macrostomum* is the
700 origin of a second female genital opening. The phylogeny suggests that a second female genital
701 opening has evolved at least four times independently within the genus (see SI Female openings for
702 a more detailed discussion). In all species, the novel second opening is associated with a muscular
703 bursa that could allow cryptic female choice, since it might eject sperm through muscular contraction.
704 Such contraction is also at play during the suck behaviour, where, at least in *M. hamatum*, sperm can

705 be seen to be ejected from the antrum even before the worm places its mouth on the female genital
706 opening (pers. comm. P. Singh).
707 In summary, our findings document a dynamic evolutionary history of male-female coevolution
708 driving frequent innovations. Such coevolution does not only lead to trait diversification, but likely
709 also drives the frequent origin of traumatic insemination, because it allows donors to overcome pre-
710 and postcopulatory choice and/or resistance mechanisms of the recipient. The drastic and repeatable
711 morphological changes associated with traumatic insemination indicate a shift in functional
712 constraints on sperm morphology and function, which are presumably not unique to these flatworms,
713 and which should therefore also be studied in gonochoristic models for traumatic insemination. Such
714 studies will allow us to disentangle specific and general factors advancing our general understanding
715 of sperm form and function.

716 # Material and Methods

717 ## Field collections and documentation

718 Almost all specimens were collected from the field in freshwater, brackish or marine habitats, either
719 from sediment samples or from water plants (details on all sampled specimens and their
720 measurements in **Tab S2**). We documented specimens extensively with digital photomicrography, as
721 previously described [41, 77, 84], using light microscopes (Leica DM2500, Olympus BH2, Leitz
722 Diaplan, Zeiss Axioscope 5) with differential interference contrast (DIC) and equipped with digital
723 cameras (Sony DFW-X700, Sony DFK41 and Ximea xiQ). We collected both images and videos at
724 various magnifications (40x to 1000x), documenting the general habitus and details of internal organs,
725 which is possible due to the small size and high transparency of these organisms. To document sperm
726 morphology we amputated a worm's tail slightly anterior of the seminal vesicle, ruptured the seminal
727 vesicle (as described in [111]), and documented the released sperm in a smash preparation using DIC
728 (and sometimes also phase-contrast microscopy). When possible, we prepared whole-mount
729 permanent preparations of these amputated tails to preserve a physical specimen of the male
730 intromittent organ, the stylet [41, 77]. Finally, we preserved the entire animal, or its anterior portion
731 when amputated, for molecular analysis, in either RNAlater solution (Sigma, stored at 4°C up to a
732 few weeks and then at -80°C) or in absolute ethanol (stored cool for up to a few weeks and then at -
733 20°C).

734 ## Morphological data

735 To characterise morphology, we collected both quantitative (Q) and categorical (C) data from the
736 detailed images and videos of the collected specimens (or from the taxonomical descriptions of the
737 few species we did not collect ourselves). Categorical data were determined on a per species basis,
738 while quantitative data were taken per individual. We measured body size (Q) as the total body area
739 and either measured or scored various aspects of the stylet (Q: length, curviness, width of the proximal

740 opening, width of the distal opening, and asymmetry of the distal thickening; C: sharpness of the
741 distal thickening), the sperm (Q: total length, bristle length; C: sperm bristle state, presence of a brush,
742 and presence of a velum) and antrum (Q: number of genital openings; C: antrum thickness, presence
743 and thickness of anterior cellular valve, antrum chamber complexity, and an overall compound
744 measure of antrum complexity). We refer the reader to the SI Morphology section for detailed
745 explanations of these measures. Morphometric analyses were performed using the software ImageJ
746 (version 1.51w) and the plugin ObjectJ (version 1.04r), which allows marking structures in the
747 original images in a non-destructive manner. The pixel length of structures was converted into µm,
748 by calibrating the different microscope setups using a stage micrometre. For comparative analysis we
749 transformed body area ($\log_{10}$ of the square-root) and $\log_{10}$ transformed all linear measures (stylet
750 length, width of the proximal opening, width of the distal opening, sperm length, and bristle length).
751 The sample sizes for all quantitative measurements are given in **Tab S1** and species averages in Tab
752 S9.

753 ## Sequence data generation

754 We extracted both DNA and RNA from the RNAlater samples using the Nucleospin XS Kit in
755 combination with the Nucleospin RNA/DNA Buffer Set (Macherey-Nagel), and we extracted DNA
756 from the ethanol samples using the DNeasy Blood and Tissue kit (Qiagen, Germany). Extracted DNA
757 and RNA was stored at -80°C. We amplified a partial *28S rRNA* sequence from DNA samples using
758 PCR primers ZX-1 and 1500R and, for some fragments, additional nested PCR using primers ZX-1
759 and 1200R, or 300F and 1500R, with polymerases and cycling conditions as previously described
760 [41, 61]. We sequenced the resulting fragments from both sides using the PCR primers (Microsynth,
761 Switzerland), assembled them in Geneious (v 11.1.5) with the built-in assembler (using the Highest
762 sensitivity setting), with minor manual trimming and correction. For some sequences, we obtained
763 additional sequences using internal primers 1090F, ECD2 (both [41]).

764 To generate the RNA-Seq library for *M. clavituba* we extracted RNA from 40 pooled animals using
765 Tri™ reagent (Sigma) and then prepared the library using the TruSeq® Stranded mRNA kit
766 (Illumina). And to generate the RNA-Seq libraries for all other selected RNA samples, we used
767 SMART-Seq v4 (Clontech Laboratories, Inc.) in combination with the Nextera XT DNA library
768 preparation kit (Illumina). When at least 5ng total RNA was available, we performed the SMART-
769 Seq v4 protocol with 12 preamplification steps and otherwise we used 1ng and performed 15
770 preamplification steps. Libraries were checked for quality using a Fragment Analyzer (Agilent) and
771 then sequenced as 101 paired-end reads on the HiSeq2500 platform (using the HiSeq® SBS Kit v4,
772 Illumina) at the Genomics Facility Basel of the University of Basel and the Department of Biosystems
773 Science and Engineering of the ETH Zürich.

774 Species delimitation

775 Most collected specimens could not be assigned to a taxonomically described *Macrostomum* species
776 (http://turbellaria.umaine.edu) [112] and are therefore likely new to science. We present
777 transcriptome-level information for most species but could not conduct RNA-Seq on all >1600
778 collected specimens. We, therefore, relied on morphology and the partial *28S rRNA* sequences for
779 species assignment since this fragment is widely used as a DNA barcode for flatworms (e.g. [77, 113–
780 115]. We constructed haplotype networks from the partial *28S rRNA* sequences using the TCS
781 algorithm [116] implemented in the TCS software [117] and chose to delimit species with >3
782 mutational differences in the network. Such a difference in this *28S rRNA* fragment indicates distinct
783 species among microturbellarians [115], but it is insufficient to clearly distinguish recently diverged
784 species within *Macrostomum* [61]. Additional markers like COI are frequently used to detect recent
785 divergence (e.g. [41, 77]), but despite considerable efforts, we were unable to develop universal
786 primers (a common issue in flatworms, see e.g. [118]) and individual primer optimisation, as in [61],
787 was not feasible here. Instead, we chose to also delimit species with ≤3 differences in this *28S rRNA*
788 fragment if they showed clear diagnostic differences in morphology. We thus err on the side of

789 lumping specimens, with species with shallow molecular and no diagnostic morphological divergence
790 being assigned to the same operational species. We provide haplotype networks accompanied by
791 drawings of the diagnostic features for all species (see SI Haplotype networks).
792 When the morphology of a species was diagnostic, we sequenced several specimens, when possible
793 from different sample locations, to confirm that they were indeed molecularly similar and then
794 assigned additional specimens based on morphology only. When no unambiguous diagnostic traits
795 could be defined (as was the case for many species of the hypodermic clade) we sequenced all
796 specimens collected for molecular assignment. We used 668 sequences generated for this study (604
797 sequences, Accessions: MT428556-MT429159) or from public databases (64 sequences),
798 representing the available diversity across the genus. We also included 15 sequences from seven
799 species of our chosen outgroup genus *Psammomacrostomum*. We aligned sequences using MAFFT
800 („—genafpair –maxiterate 1000“) and generated haplotype networks for the recovered clades. We
801 removed all columns that contained at least one gap before running TCS, leaving us with an alignment
802 with 787 sites and 385 variable bases. We thus ignore indels to avoid the generation of cryptic species
803 solely based on these, since scoring indels is non-trivial, and they are frequently treated as missing
804 data [119].

805 Phylogenetics

806 We used 134 transcriptomes representing 105 species, including four distant outgroups,
807 *Haplopharynx rostratum*, *Microstomum lineare*, *Myozonaria bistylifera*, and *Karlingia* sp. 1, three
808 species from the sister genus, *Psammomacrostomum* (see also [77]), and 98 *Macrostomum* species in
809 the phylogenomic analysis. This included the four publicly available high-quality transcriptomes of
810 *M. hystrix*, *M. spirale*, *M. pusillum* [120], and *M. lignano* [121, 122], as well as 130 *de novo*
811 assembled transcriptomes. Transcriptomes were assembled as previously described [120] and were
812 mostly derived from whole single specimens (and a few from anterior fragments only, which may
813 reduce the transcriptome repertoire), while nine were generated by combining RNA-Seq data sets

814 from several animals or pooling animals that were collected at the same location and assigned to the
815 species based on our taxonomic expertise into one sample (for details on the transcriptomes used see
816 **Tab S8**). We assessed transcriptome quality using TransRate (version 1.0.2, [123]), which maps the
817 reads back to the assembly and calculates mapping metrics, and BUSCO (version 2.0, [124]), which
818 searches for the presence of a curated set of core conserved genes. Specifically, we ran the BUSCO
819 analysis with the metazoan dataset consisting of 978 genes (version uploaded 2016-11-01). These
820 BUSCO scores were also used to select one representative transcriptome when multiple
821 transcriptomes were available for a species (see below). We determined the empirical insert size of
822 our libraries by mapping the reads to the assemblies using SNAP (version 1.0, [125]) and then
823 extracting the mean insert size using Picard (version 2.20.2).
824 To infer a set of orthologous genes (orthologs) we predicted open reading frames (ORFs) for each
825 transcriptome using TransDecoder (version 5.3.0 [126]) with Pfam searches (version 32.0) to retain
826 transcripts with predicted proteins and kept only one ORF per transcript using the "--
827 single_best_only" option. We then clustered predicted proteins with at least 99.5% sequence identity
828 using the CD-HIT clustering algorithm (version 4.7, [127]). The amino acid sequences where then
829 processed with OrthoFinder (version 2.2.6, [128]) using the „-os" option to perform a length-adjusted
830 reciprocal BLAST searches followed by MCL clustering. We processed the resulting set of
831 homologous genes (homogroups) using modified scripts from the phylogenomic dataset construction
832 workflow [129]. We aligned all homogroups that contained at least 10 species using MAFFT (version
833 7.310, „–genafpair –maxiterate 1000" [130]), inferred the best substitution model with ModelFinder
834 [131], and the gene tree using IQ-TREE (version 1.5.5, [66], command: "-mset DCMut, JTTDCMut,
835 LG, mtZOA, PMB, VT, WAG –mfreq FU,F –mrate G"). Then we trimmed the gene trees using
836 "trim_tips.py" to remove tip branches that were longer than two substitutions per site and
837 "mask_tips_by_taxonID_transcripts.py" to remove monophyletic paralogs by choosing the sequence
838 with the best representation in the alignment. We split off subtrees with long internal branches using
839 "cut_long_internal_branches.py" and inferred orthologs using the rooted outgroup method in

840 "prune_paralogs_RT.py". This method uses known outgroup taxa to root the phylogenies, which then
841 allows to infer the history of speciation and duplication and extract the most inclusive set of orthologs.
842 We defined *Haplopharynx rostratum*, *Microstomum lineare*, *Myozonaria bistylifera*, and
843 *Karlingia sp. 1* as the outgroup and all *Macrostomum* and *Psammomacrostomum* as an ingroup
844 (following the phylogeny of [77]), since the algorithm does not include the defined outgroup in the
845 output, and we then used *Psammomacrostomum* to root our final ortholog trees. Next, we realigned
846 the orthogroups using MAFFT and trimmed the alignment with ZORRO [132], discarding any
847 columns in the alignment with a score of less than five and filtering alignments that were shorter than
848 50 amino acids after trimming. Finally, we inferred ortholog gene trees with 100 non-parametric
849 bootstraps with IQ-TREE, by inferring the best fitting model „-mset DCMut, JTTDCMut, LG,
850 mtZOA, PMB, VT, WAG -mfreq FU,F -mrate E,I,G,I+G“. These best fitting substitution models
851 were later also used for the partitioned maximum-likelihood analysis.
852 We generated two gene matrices, one matrix containing many genes but a relatively moderate
853 occupancy (called L for low occupancy) and one with a lower gene number but a higher occupancy
854 (called H for high occupancy, **Tab 2**). We conducted most analyses on the H alignment for
855 computational tractability and since missing data can have a negative influence on tree inference,
856 particularly when using Bayesian methods ([133], but see [134]), and only the less computationally
857 demanding summary and maximum-likelihood methods were also applied to the L alignment. So for
858 both alignments, we calculated a maximum likelihood species phylogeny using IQ-TREE ("L-IQ-
859 TREE" and "H-IQ-TREE") with a partition for each gene and using the best substitution model for
860 each gene (see above). We calculated 1000 ultrafast bootstraps and conducted an approximate-
861 likelihood ratio test to assess branch support. We inferred Bayesian phylogenies using ExaBayes
862 (version 1.5, [68]) for the H alignment ("H-ExaBayes") with partitions for each gene, equal prior
863 probability on all available amino acid substitution models, and with gamma models for all partitions.
864 We ran four independent chains retaining every 500th iteration and discarding the first 365,000
865 iterations as burn-in. We terminated the analysis after 1.46 million generations since the average

866 deviation of split frequencies between all the chains was below 1%, indicating convergence. We
867 further assessed convergence using Gelman's R of the likelihoods with the R package coda [136],
868 which showed three chains had converged, while one appeared stuck on a local peak. Since all chains
869 quickly converged on the same topology, the local peak probably occurs due to differences in the
870 substitution models applied, with the HIVB model being present at a low rate in the three converged
871 chains, but being absent in the fourth. We combined the three converged chains, discarded the fourth
872 and calculated a consensus tree using quadratic path distance optimisation (using the ls.consensus
873 function in the R package phytools).
874 To account for potential issues caused by model misspecification, we also performed an unpartitioned
875 analysis using the CAT model implemented in PhyloBayes (version 1.5, [69]). Because a full GTR
876 model of the amino acids was too parameter rich, we ran the tool on the DNA coding sequence of the
877 H alignment and fit the CAT+GTR model ("H-PhyloBayes"). Two chains were run in parallel on 400
878 CPUs for two weeks. Due to the high cost of the analysis, we terminated the run after 23,311
879 iterations, at which point the chains showed an identical topology (after removal of 10,000 iterations
880 as a burn-in). At this point the realised difference in the likelihoods between the two H-PhyloBayes
881 chains was high (0.21 with an ESS of 858) suggesting the chains had not converged. However,
882 Gelman diagnostics for the likelihoods suggested convergence. Our chains could potentially be at a
883 local peak where the hypodermic clade is paraphyletic, possibly due to poor mixing, potentially
884 biasing the results. Therefore, we discuss the H-PhyloBayes phylogeny, but exclude it from the
885 comparative analysis.
886 To construct phylogenies while accounting for potential incomplete lineage sorting, we ran the quartet
887 based method implemented in ASTRAL-III (version: 5.6.1, [67]) on both alignments ("L-ASTRAL"
888 and "H-ASTRAL"). We assessed the level of gene tree – species tree conflict at each node of the
889 phylogeny using the quartet support score, which gives the proportion of quartet trees induced by the
890 gene trees that are supporting the species tree topology as opposed to the two possible alternatives
891 [67]. Strong support for the species tree partition can be interpreted as little disagreement between

892 the gene trees, while support for the alternate topologies indicates strong gene tree – species tree
893 conflict.

894 Furthermore, we chose representative *28S rRNA* sequences from the haplotype network analysis to
895 infer phylogenetic placement for species without a transcriptome. For species with a transcriptome,
896 we mostly chose the *28S rRNA* sequence derived from the same specimen (for exceptions see
897 **Tab S8**). We aligned the sequences using MAFFT ("--maxiterate 1000 –globalpair"), trimmed the
898 start and end using trimAl ("–nogaps –terminalonly" [137]) and determined the best substitution
899 model using ModelFinder with the BIC criterion. We then combined this alignment with the H amino
900 acid alignment, and analysed it with the best fitting substitution model using IQ-TREE as described
901 above (referred to as "C-IQ-TREE", called C for combined). For comparative analysis, we
902 transformed the phylogenies (C-IQ-TREE, H-IQ-TREE and H-ExaBayes) to be ultrametric and with
903 a root depth of 1 using the penalized marginal likelihood approach [138] implemented in the software
904 TreePL [139].

905 We performed all follow-up analyses on the H-IQ-TREE and the H-ExaBayes phylogenies to explore
906 possible effects of phylogenetic uncertainty and included the C-IQ-TREE phylogeny to incorporate
907 more species. We pruned the phylogenies to include one representative tip per species, choosing the
908 transcriptome with the best BUSCO score. We present the results obtained with all three phylogenies,
909 but primarily discuss the ones obtained with the C-IQ-TREE phylogeny, since all results are
910 quantitatively similar and qualitatively identical.

911 After the above analyses were completed, we discovered that some transcripts of the RNA-Seq
912 libraries constructed with the SMART-Seq v4 cDNA kit contained cDNA synthesis primer
913 sequences. We did not remove these primers before transcriptome assembly since i) the manufacturer
914 specifically states they should not occur in RNA-Seq reads if used in combination with the Nextera
915 XT DNA library preparation kit (Appendix C in SMART-Seq v4 Ultra Low Input RNA Kit for
916 Sequencing User Manual, Takara Bio Inc. available at: https://www.takarabio.com/assets/a/114825)
917 and ii) because the relevant primer sequence is proprietary (both confirmed by Takara EU tech

support in November 2020), so that we initially did not have access to its sequence. We only discovered the offending primer sequence due to ongoing work on two *Macrostomum* genome projects. Because the analyses presented here had at this point used approximately 650,000 CPU hours of computation, and since the effect of the primer was likely small, we elected to perform some follow-up analyses to determine how robust our results were to its removal, rather than opting for a complete re-assembly and re-analysis of all the data. As we outline in SI Primer removal, the removal of the cDNA synthesis primer sequences had little effect on the topology and branch lengths of L-IQ-TREE, H-IQ-TREE and C-IQ-TREE and, therefore, we present the results based on the original alignments.

Frequent origins of hypodermic insemination

The original definitions of the mating syndromes integrated both morphological and behavioural traits [41]. Because we here lacked behavioural data for most species, we adapted the definitions, relying instead on several morphological traits and the observed received sperm location only to derive the inferred mating syndrome (Tab 3). We assigned species to the hypodermic mating syndrome if we exclusively found hypodermic received sperm, since this represents strong evidence for hypodermic insemination, as opposed to species where we observed both hypodermic sperm and received sperm in the female antrum, which we classify as intermediate (Tab 3). Moreover, because hypodermic sperm can be difficult to observe, especially in species with low investment into sperm production, we also assigned species that lacked received sperm observations to the hypodermic mating syndrome based on their morphology alone, namely when they had a simple antrum, a sharp stylet, and absent or reduced sperm bristles (**Tab 3**). And while observing received sperm in the female antrum may not exclude occasional hypodermic insemination, it is a strong indication of the reciprocal mating syndrome, especially when it occurs in a species with a blunt stylet. We, therefore, assigned all species with received sperm in the antrum and a blunt stylet to the reciprocal mating syndrome (**Tab 3**). And since some reciprocally mating species also have a sharp stylet (e.g. *M. spirale*), which could possibly

943 wound the partner internally during mating (pers. obs.), we also assigned these species to the
944 reciprocal mating syndrome, provided that we observed received sperm in the antrum, and that they
945 had sperm with bristles (**Tab 3**). These assignments based on morphology alone are supported by our
946 analysis of correlated evolution, showing a strong association between the received sperm location
947 and both sperm bristle state and antrum type, respectively (see Results). The inferred mating
948 syndrome is therefore a more inclusive classification of hypodermic insemination compared to an
949 assignment based on received sperm location alone.
950 We estimated ancestral states of the mating syndrome and three reproductive traits linked to it, namely
951 received sperm location, sperm bristle state, and antrum state. First, we used binary scorings (see SI
952 Morphology), equivalent to how they were used in the tests for correlated evolution (see below).
953 However, since we predicted that losses/reductions of the trait would transition via an intermediate
954 state, we also reconstructed ancestral states with the inferred mating syndrome, received sperm
955 location and sperm bristle state scored as trinary states. We estimate the history of transitions using
956 stochastic character mapping [140] with the R package phytools [141]. We determined the
957 appropriate transition matrix for reconstruction by fitting MK-models with either all state transitions
958 with equal rates (ER), with symmetric rates (SYM), with all rates different (ARD), and with a model
959 without the possibility of gains once the trait is lost (Dollo). For traits with trinary states, we
960 additionally fit an ordered model, where transitions have to go via the intermediate state (ORD) and
961 an ordered Dollo model without the possibility of gains once the trait is completely lost, but allowing
962 transitions back from the intermediate state (ORD-Dollo). We reconstructed ancestral states for all
963 models with a corrected AIC weight >0.15 (Table 3). We used the fully Bayesian implementation of
964 stochastic character mapping with a gamma prior on each transition ($\alpha = 1$, $\beta = 1$, this results in a low
965 prior on the number of transitions) and reconstructed 1000 character histories (10.000 iterations burn-
966 in followed by 10,000 iterations and retaining every 10th character history). We summarised the
967 number of transitions as the average number of changes as well as the 95% credible interval.

968 ## Correlated evolution

969 We performed a number of tests of correlated evolution to ask if the numerous convergent changes
970 in received sperm location, sperm bristle state and antrum state were evolutionarily dependent. But
971 since we do not have direct observations of received sperm in all species, we first conducted a
972 correlation test between sperm bristle state and received sperm location, and then tested for correlated
973 evolution between both of these variables and the antrum type. We scored all traits as binary and
974 applied Pagel's correlation test [142] as implemented in BayesTraits3 (available at
975 http://www.evolution.rdg.ac.uk/BayesTraitsV3.0.2/BayesTraitsV3.0.2.html). This test compares the
976 marginal likelihood of a model where the transition probability of the first trait depends on the state
977 of the second trait with a model where the two traits evolve independently. For all analysis we ran
978 four independent MCMC chains for 510 million iterations, discarding the first 10 million iterations
979 as burn-in and retaining every 1000th iteration. We calculated the marginal likelihood of the models
980 using the stepping stone sampler of BayesTraits3 with 1000 power posteriors estimated with 10,000
981 iterations each. We assessed convergence of the chains by calculating Gelman's R using the coda R
982 package [136] and upon confirming convergence merged the chains for further analysis. To evaluate
983 sensitivity to the prior, we ran all analyses with a uniform prior (U 0 100), an exponential prior (exp
984 10) and a reversible-jump hyperprior with a gamma distribution between 0 and 1 for both the rate
985 prior and the hyperprior (rjhp gamma 0 1 0 1). Models were compared with Bayes factors using the
986 marginal likelihoods calculated by the stepping stone sampler (i.e. $BF=2(logLH_{dependent} -$
987 $logLH_{independent})$). To assess the influence of the phylogeny we conducted these tests on three different
988 phylogenies. This setup resulted in 54 model runs consisting of 216 MCMC chains (three trait pairs
989 x three priors x three topologies x four chains for the independent and the dependent model; see also
990 the Correlated evolution section in the Supporting Information). The number of species included was
991 largest for the correlation between sperm bristle state and antrum type (C-IQ-TREE: 124; H-IQ-TREE
992 & H-ExaBayes: 95), and similar for received sperm location and antrum type (C-IQ-TREE: 100; H-

993 IQ-TREE & H-ExaBayes: 77) and received sperm location and sperm bristle state (C-IQ-TREE: 101;
994 H-IQ-TREE & H-ExaBayes: 76).

995 Hypodermic insemination and convergence in morphospace

996 We conducted a multivariate analysis to investigate whether the convergent evolution of hypodermic
997 insemination is associated with changes in a variety of reproductive traits (see SI Morphology, and
998 Tables A1-2 and Figures A1-3 therein). For this we summarized all our data on stylet, sperm and
999 antrum morphology (including both quantitative and categorical data) using principal component
1000 analysis. Since regular principal component analysis assumes independence of observations, an
1001 assumption violated by the phylogenetic relationships of species [143], we calculated a
1002 phylogenetically corrected principal component (pPCA), using the phyPCA function in phytools with
1003 the lambda model. Since we combined data with different scales, we used the correlation matrix for
1004 all calculations. When discussing loadings of principal components we apply an aggressive threshold
1005 of ±0.5, since although this results in erosion of power, it keeps false-positive rate within expectations
1006 [144].

1007 Hypodermic insemination and sperm morphology

1008 To test the influence of hypodermic insemination on sperm length, we performed phylogenetically
1009 corrected ordinary least squared regression (PGLS) with the *gls* function in the R package *nlme*
1010 (version 3.1). We used *gls* because it allowed us to simultaneously incorporate phylogenetic signal in
1011 the residuals and account for variation in the number of measured specimens by using the sample size
1012 of the response as weights. We determined the best fitting evolutionary model for the covariance in
1013 the residuals by comparing corrected AIC of PGLS fitted with Brownian motion, lambda or Ornstein-
1014 Uhlenbeck models. We assessed if the assumptions of the PGLS were met by checking the
1015 distributions of the phylogeny-corrected residuals for normality and profiled the likelihood of the
1016 parameter of the correlation structure (i.e. lambda or alpha). Since R-squared values are problematic

1017 for PGLS models [145] we calculated R_{pred} [146] to show model fits. As predictors, we used the
1018 binary traits included in the test of correlated evolution (received sperm location, sperm bristle state
1019 and antrum state) since they all are strong indicators of hypodermic insemination. Moreover, we also
1020 included the inferred mating syndrome as a predictor, but coded it as binary (hypodermic and
1021 reciprocal), and excluding the intermediate syndrome due to the low sample size of this group.
1022 Analysing all four of these predictors is somewhat redundant, but while received sperm location is
1023 the most direct evidence for hypodermic insemination it results in a reduced sample size (see above)
1024 and the other predictors allow the inclusion of more species.

1025 Coevolution of male and female genitalia

1026 If male and female genitalia coevolve, we expect correlations in aspects of their morphology across
1027 species. Ideally, this is detected by identifying homologous male and female structures in all species
1028 and correlating their shape evolution (e.g. [107]). However, the stylets within the reciprocal clade are
1029 highly variable, making the identification and placement of consistent landmarks challenging.
1030 Similarly, capturing the morphology of the antrum is challenging because these soft internal
1031 structures are highly transparent in live specimens. And while the antrum can be studied in
1032 histological sections, it can appear distorted and contracted due to the fixation, making it difficult to
1033 accurately measure length or volume. With these caveats in mind, we independently summarised
1034 male and female genital complexity using pPCAs (see above) and then performed a PGLS regression
1035 (see above) between the first principal components of each pPCA. We used five stylet traits (stylet
1036 length, curviness, width of proximal opening, width of distal opening, and distal asymmetry) and four
1037 antrum traits (thickness, cellular valve, chamber complexity and number of genital openings). We
1038 performed the PGLS regression both across all species and as well as only including species
1039 categorised as showing the reciprocal mating syndrome, since the species with the hypodermic mating
1040 syndrome were nearly invariant.

Acknowledgment

We thank the numerous people that have helped with field work. Especially, we are grateful for the help of, in no particular order, Werner Armonies, Benny Glasgow, Mohamed Charni, Edith Zemp, Bernhard Egger, Peter Ladurner, Gregor Schulte, Floriano Papi, Kazuya Kobayashi, Christopher Laumer, Wim Willems, Tom Artois, Christian Lott, Miriam Weber, Ana-Maria Leal-Zanchet, Kaja Wasik, Mariana Adami, Walter Salzburger, Adrian Indermaur, Bernd Egger, Fabrizia Ronco, Heinz Büscher, Victoria Huwiler, Philipp Kaufmann, Michaela Zwyer, Stefanie von Fumetti, Joe Ryan, Mark Q. Martindale, Marta Chiodin, John Evans, Leigh Simmons, Mauro Tognon, Piero Tognon, Cristiano Tognon, Pragya Singh, Nikolas Vellnow, Christian Felber, Ulf Jondelius, Sarah Atherton, Tim Janicke, Georgina Rivera-Ingraham, Ben Byrne, Yvonne Gilbert, Rod Watson, Jochen Rink, Miquel Vila-Fare, Helena Bilandžija, and Sasho Trajanovski. We thank Katja Eschbach of the Genomics Facility Basel for preparing and sequencing RNA-Seq libraries. We thank Peter Fields and Lukas Zimmermann for IT advice. We thank Jürgen Hottinger, Daniel Lüscher and Yasmin Picton for administrative and technical support. We thank Dita Vizoso for the use of sperm and stylet drawings for some of the previously described species and for providing inspiration for the new drawings. We thank Yu Zhang and his collaborators for kindly providing specimens of *M. baoanensis*. We thank Nick Goldman and Ziheng Yang for organising the summer school on Computational Molecular Evolution, which has helped and inspired the first author to explore phylogenetics. Calculations were performed, in part, at sciCORE (http://scicore.unibas.ch/) scientific computing centre at the University of Basel.

Funding

This work was supported by Swiss National Science Foundation (SNSF) research grants 31003A_162543 and 310030_184916 to LS.

1064 ## Competing Interests

1065 All Authors declare that they have no competing interests.

1066 ## Data availability

1067 The raw sequencing data generated for this study are available in the NCBI
1068 Sequence Read Archive repository with the following accession: PRJNA635941. The partial *28S*
1069 *rRNA* sequence are available on NCBI with the following accessions: MT428556-MT429159.
1070 Extensive image and video material of all documented specimens are deposited on Zenodo at:
1071 10.5281/zenodo.4482135. Transcriptome assemblies, gene alignments and phylogenetic trees are
1072 deposited on Zenodo at: 10.5281/zenodo.4543289.

1073 # References

1074 1. Bateman AJ. Intra-sexual selection in *Drosophila*. Heredity. 1948;2:349–68.

1075 2. Arnold SJ. Bateman's principles and the measurement of sexual selection in plants and animals.
1076 Am Nat. 1994;144:S126–49.

1077 3. Janicke T, Häderer IK, Lajeunesse MJ, Anthes N. Darwinian sex roles confirmed across the animal
1078 kingdom. Sci Adv. 2016;2:e1500983–e1500983.

1079 4. Parker GA. The sexual cascade and the rise of pre-ejaculatory (Darwinian) sexual selection, sex
1080 roles, and sexual conflict. Cold Spring Harb Perspect Biol. 2014;6:a017509–a017509.

1081 5. Puurtinen M, Ketola T, Kotiaho JS. The Good-Genes and Compatible-Genes Benefits of Mate
1082 Choice. Am Nat. 2009;174:741–52.

1083 6. Arnqvist G, Nilsson T. The evolution of polyandry: multiple mating and female fitness in insects.
1084 Anim Behav. 2000;60:145–64.

1085 7. Hosken DJ, Stockley P. Benefits of Polyandry: A Life History Perspective. In: Macintyre RJ, Clegg
1086 MT, editors. Evolutionary Biology. Boston, MA: Springer US; 2003. p. 173–94. doi:10.1007/978-1-
1087 4757-5190-1_4.

1088 8. Arnqvist G, Rowe L. Sexual conflict. Princeton, N.J: Princeton University Press; 2005.

1089 9. Parker GA. Sexual conflict over mating and fertilization: An overview. Philos Trans R Soc B Biol
1090 Sci. 2006;361:235–59.

1091 10. Rice WR. Sexually antagonistic male adaptation triggered by experimental arrest of female
1092 evolution. Nature. 1996;381:232–4.

1093 11. Arnqvist G, Rowe L. Antagonistic coevolution between the sexes in a group of insects. Nature.
1094 2002;415:787–9.

1095 12. Charnov EL. Simultaneous hermaphroditism and sexual selection. Proc Natl Acad Sci U S A.
1096 1979;76:2480–4.

1097 13. Birkhead TR, Pizzari T. Evolution of sex: postcopulatory sexual selection. Nat Rev Genet.
1098 2002;3:262–73.

1099 14. Wedell N, Hosken DJ. The evolution of male and female internal reproductive organs in insects.
1100 In: Leonard JL, Córdoba-Aguilar A, editors. The evolution of primary sexual characters in animals.
1101 Oxford ; New York: Oxford University Press; 2010.

1102 15. Morrow EH, Arnqvist G. Costly traumatic insemination and a female counter-adaptation in bed
1103 bugs. Proc R Soc B Biol Sci. 2003;270:2377–81.

1104 16. Morrow EH, Arnqvist G, Pitnick S. Adaptation versus pleiotropy: why do males harm their mates?
1105 Behav Ecol. 2003;14:802–6.

1106 17. Lange R, Reinhardt K, Michiels NK, Anthes N. Functions, diversity, and evolution of traumatic
1107 mating: function and evolution of traumatic mating. Biol Rev. 2013;88:585–601.

1108 18. Schärer L, Janicke T, Ramm SA. Sexual conflict in hermaphrodites. Cold Spring Harb Perspect
1109 Biol. 2015;7:a017673.

1110 19. Reinhardt K, Naylor R, Siva-Jothy MT. Reducing a cost of traumatic insemination: female
1111 bedbugs evolve a unique organ. Proc R Soc B Biol Sci. 2003;270:2371–5.

1112 20. Reinhardt K, Anthes N, Lange R. Copulatory wounding and traumatic insemination. Cold Spring
1113 Harb Perspect Biol. 2015;7:a017582.

1114 21. Benoit JB, Jajack AJ, Yoder JA. Multiple traumatic insemination events reduce the ability of bed
1115 bug females to maintain water balance. J Comp Physiol B. 2012;182:189–98.

1116 22. Tatarnic NJ. Traumatic Insemination and Copulatory Wounding. In: Reference Module in Life
1117 Sciences. Elsevier; 2018.

1118 23. Tatarnic NJ, Cassis G, Siva-Jothy MT. Traumatic insemination in terrestrial arthropods. Annu
1119 Rev Entomol. 2014;59:245–61.

1120 24. Kathirithamby J, Hrabar M, Delgado JA, Collantes F, Dötterl S, Windsor D, et al. We do not
1121 select, nor are we choosy: reproductive biology of Strepsiptera (Insecta). Biol J Linn Soc.
1122 2015;116:221–38.

1123 25. Peinert M, Wipfler B, Jetschke G, Kleinteich T, Gorb SN, Beutel RG, et al. Traumatic
1124 insemination and female counter-adaptation in Strepsiptera (Insecta). Sci Rep. 2016;6:25052.

1125 26. Stutt AD, Siva-Jothy MT. Traumatic insemination and sexual conflict in the bed bug *Cimex*
1126 *lectularius*. Proc Natl Acad Sci. 2001;98:5683–7.

1127 27. Siva-Jothy M t. Trauma, disease and collateral damage: conflict in cimicids. Philos Trans R Soc
1128 B Biol Sci. 2006;361:269–75.

1129 28. Michiels NK, Newman LJ. Sex and violence in hermaphrodites. Nature. 1998;391:647–647.

1130 29. Sluys R. Sperm resorption in triclads (Platyhelminthes, Tricladida). Invertebr Reprod Dev.
1131 1989;15:89–95.

1132 30. Koene JM. Tales of two snails: sexual selection and sexual conflict in Lymnaea stagnalis and
1133 Helix aspersa. Integr Comp Biol. 2006;46:419–29.

1134 31. Koene JM, Montagne-Wajer K, Roelofs D, Ter Maat A. The fate of received sperm in the
1135 reproductive tract of a hermaphroditic snail and its implications for fertilisation. Evol Ecol.
1136 2009;23:533–43.

1137 32. Parker GA. Sperm competition and the evolution of ejaculates: towards a theory base. In: Sperm
1138 competition and sexual selection. T.R. Birkhead and A.P. Møller. San Diego: Academic Press; 1998.
1139 p. 3–54.

1140 33. Řezáč Milan. The spider *Harpactea sadistica*: Co-evolution of traumatic insemination and
1141 complex female genital morphology in spiders. Proc R Soc B Biol Sci. 2009;276:2697–701.

1142 34. Parker GA. Sperm competition games: raffles and roles. Proc R Soc Lond B Biol Sci.
1143 1990;242:120–6.

1144 35. Charnov EL. Sperm competition and sex allocation in simultaneous hermaphrodites. Evol Ecol.
1145 1996;10:457–62.

1146 36. Greeff JM, Parker GA. Spermicide by females: what should males do? Proc R Soc B Biol Sci.
1147 2000;267:1759–63.

1148 37. van Velzen E, Scharer L, Pen I. The effect of cryptic female choice on sex allocation in
1149 simultaneous hermaphrodites. Proc R Soc B Biol Sci. 2009;276:3123–31.

1150 38. Schärer L, Pen I. Sex allocation and investment into pre- and post-copulatory traits in
1151 simultaneous hermaphrodites: the role of polyandry and local sperm competition. Philos Trans R Soc
1152 B Biol Sci. 2013;368:20120052–20120052.

1153 39. Vizoso DB, Gunde Rieger, Lukas Schärer. Goings-on inside a worm: functional hypotheses
1154 derived from sexual conflict thinking. Biol J Linn Soc. 2010;99:370–83.

1155 40. Schärer L, Janicke T. Sex allocation and sexual conflict in simultaneously hermaphroditic
1156 animals. Biol Lett. 2009;5:705–8.

1157 41. Schärer L, Littlewood DTJ, Waeschenbach A, Yoshida W, Vizoso DB. Mating behavior and the
1158 evolution of sperm design. Proc Natl Acad Sci. 2011;108:1490–5.

1159 42. Parker GA. Selection on non-random fusion of gametes during the evolution of anisogamy. J
1160 Theor Biol. 1978;73:1–28.

1161 43. Parker GA. Why are there so many tiny sperm? Sperm competition and the maintenance of two
1162 sexes. J Theor Biol. 1982;:281–94.

1163 44. Parker GA. Sperm competition games: sperm size and sperm number under adult control. Proc R
1164 Soc Lond B Biol Sci. 1993;253:245–54.

1165 45. Immler S, Pitnick S, Parker GA, Durrant KL, Lüpold S, Calhim S, et al. Resolving variation in
1166 the reproductive tradeoff between sperm size and number. Proc Natl Acad Sci. 2011;108:5325–30.

1167 46. Michiels NK. Mating conflicts and sperm competition in simultaneous hermaphrodites. In: Sperm
1168 Competition and Sexual Selection. T.R. Birkhead and A.P. Møller. Elsevier; 1998. p. 219–54.

1169 47. Anthes N, Putz A, Michiels NK. Sex role preferences, gender conflict and sperm trading in
1170 simultaneous hermaphrodites: a new framework. Anim Behav. 2006;72:1–12.

1171 48. Anthes N. Mate choice and reproductive conflict in simultaneous hermaphrodites. In: Kappeler
1172 P, editor. Animal Behaviour: Evolution and Mechanisms. Berlin, Heidelberg: Springer Berlin
1173 Heidelberg; 2010. p. 329–57.

1174 49. Anthes N, David P, Auld JR, Hoffer JNA, Jarne P, Koene JM, et al. Bateman gradients in
1175 hermaphrodites: an extended approach to quantify sexual selection. Am Nat. 2010;176:249–63.

1176 50. Pélissié B, Jarne P, David P. Sexual selection without sexual dimorphism: Bateman gradients in
1177 a simultaneous hermaphrodite. Evolution. 2012;66:66–81.

1178 51. Michiels NK, Koene JM. Sexual selection favors harmful mating in hermaphrodites more than in
1179 gonochorists. Integr Comp Biol. 2006;46:473–80.

1180 52. Jarne P, Auld JR. Animals mix it up too: the distribution of self-fertilization among
1181 hermaphroditic animals. Evolution. 2006;60:1816–24.

1182 53. Koene JM, Schulenburg H. Shooting darts: co-evolution and counter-adaptation in
1183 hermaphroditic snails. BMC Evol Biol. 2005;5:25.

1184 54. Koene JM, Pförtner T, Michiels NK. Piercing the partner's skin influences sperm uptake in the
1185 earthworm Lumbricus terrestris. Behav Ecol Sociobiol. 2005;59:243.

1186 55. Kamimura Y. Twin intromittent organs of *Drosophila* for traumatic insemination. Biol Lett.
1187 2007;3:401–4.

1188 56. Tatarnic NJ, Cassis G. Surviving in sympatry: Paragenital divergence and sexual mimicry
1189 between a pair of traumatically inseminating plant bugs. Am Nat. 2013;182:542–51.

1190 57. Ramm SA, Vizoso DB, Schärer L. Occurrence, costs and heritability of delayed selfing in a free-
1191 living flatworm. J Evol Biol. 2012;25:2559–68.

1192 58. Ramm SA, Schlatter A, Poirier M, Schärer L. Hypodermic self-insemination as a reproductive
1193 assurance strategy. Proc R Soc B Biol Sci. 2015;282:20150660.

1194 59. Winkler L, Ramm SA. Experimental evidence for reduced male allocation under selfing in a
1195 simultaneously hermaphroditic animal. Biol Lett. 2018;14:20180570.

1196 60. Schärer L, Joss G, Sandner P. Mating behaviour of the marine turbellarian *Macrostomum* sp.:
1197 these worms suck. Mar Biol. 2004;145:373–80.

1198 61. Schärer L, Brand JN, Singh P, Zadesenets KS, Stelzer C-P, Viktorin G. A phylogenetically
1199 informed search for an alternative *Macrostomum* model species, with notes on taxonomy, mating
1200 behavior, karyology, and genome size. J Zool Syst Evol Res. 2020;58:41–65.

1201 62. Patlar B, Weber M, Temizyürek T, Ramm SA. Seminal fluid-mediated manipulation of post-
1202 mating behavior in a simultaneous hermaphrodite. Curr Biol. 2020;30:143–9.

1203 63. Weber M, Patlar B, Ramm SA. Effects of two seminal fluid transcripts on post-mating behaviour
1204 in the simultaneously hermaphroditic flatworm *Macrostomum lignano*. J Evol Biol. 2020;:jeb.13606.

1205 64. Holland B, Rice WR. Perspective: chase-away sexual selection: antagonistic seduction versus
1206 resistance. Evolution. 1998;52:1–7.

1207 65. Brand JN. Specimens from Brand et al. 2020, "Frequent origins of traumatic insemination involve
1208 convergent shifts in sperm and genital morphology". Zenodo.
1209 http://doi.org/10.5281/zenodo.XXXXX. 2020.

1210 66. Nguyen L-T, Schmidt HA, von Haeseler A, Minh BQ. IQ-TREE: a fast and effective stochastic
1211 algorithm for estimating maximum-likelihood phylogenies. Mol Biol Evol. 2015;32:268–74.

1212 67. Zhang C, Rabiee M, Sayyari E, Mirarab S. ASTRAL-III: polynomial time species tree
1213 reconstruction from partially resolved gene trees. BMC Bioinformatics. 2018;19 Suppl 6.

1214 68. Aberer AJ, Kobert K, Stamatakis A. Exabayes: Massively parallel bayesian tree inference for the
1215 whole-genome era. Mol Biol Evol. 2014;31:2553–6.

1216 69. Lartillot N, Rodrigue N, Stubbs D, Richer J. PhyloBayes MPI: Phylogenetic Reconstruction with
1217 Infinite Mixtures of Profiles in a Parallel Environment. Syst Biol. 2013;62:611–5.

1218 70. Vellnow N, Vizoso DB, Viktorin G, Schärer L. No evidence for strong cytonuclear conflict over
1219 sex allocation in a simultaneously hermaphroditic flatworm. BMC Evol Biol. 2017;17:103.

1220 71. Zadesenets KS, Vizoso DB, Schlatter A, Konopatskaia ID, Berezikov E, Schärer L, et al. Evidence
1221 for karyotype polymorphism in the free-living flatworm, *Macrostomum lignano*, a model organism
1222 for evolutionary and developmental biology. Plos One. 2016;11:e0164915.

1223 72. Robinson DF, Foulds LR. Comparison of phylogenetic trees. Math Biosci. 1981;53:131–47.

1224 73. Irisarri I, Singh P, Koblmüller S, Torres-Dowdall J, Henning F, Franchini P, et al. Phylogenomics
1225 uncovers early hybridization and adaptive loci shaping the radiation of Lake Tanganyika cichlid
1226 fishes. Nat Commun. 2018;9:3159.

1227 74. Singh P, Ballmer DN, Laubscher M, Schärer L. Successful mating and hybridisation in two
1228 closely related flatworm species despite significant differences in reproductive morphology and
1229 behaviour. Sci Rep. 2020;10:12830.

1230 75. Pleijel F, Jondelius U, Norlinder E, Nygren A, Oxelman B, Schander C, et al. Phylogenies without
1231 roots? A plea for the use of vouchers in molecular phylogenetic studies. Mol Phylogenet Evol.
1232 2008;48:369–71.

1233 76. Xin F, Zhang S-Y, Shi Y-S, Wang L, Zhang Y, Wang A-T. *Macrostomum shenda* and *M. spiriger*,
1234 two new brackish-water species of *Macrostomum* (Platyhelminthes: Macrostomorpha) from China.
1235 Zootaxa. 2019;4603:105.

1236 77. Janssen T, Vizoso DB, Schulte G, Littlewood DTJ, Waeschenbach A, Schärer L. The first multi-
1237 gene phylogeny of the Macrostomorpha sheds light on the evolution of sexual and asexual
1238 reproduction in basal Platyhelminthes. Mol Phylogenet Evol. 2015;92:82–107.

1239 78. Leasi F, Sevigny JL, Laflamme EM, Artois T, Curini-Galletti M, de Jesus Navarrete A, et al.
1240 Biodiversity estimates and ecological interpretations of meiofaunal communities are biased by the
1241 taxonomic approach. Commun Biol. 2018;1:1–12.

1242 79. Egger B, Ladurner P, Nimeth K, Gschwentner R, Rieger R. The regeneration capacity of the
1243 flatworm *Macrostomum lignano*—on repeated regeneration, rejuvenation, and the minimal size
1244 needed for regeneration. Dev Genes Evol. 2006;216:565–77.

1245 80. Maddison WP, FitzJohn RG. The unsolved challenge to phylogenetic correlation tests for
1246 categorical characters. Syst Biol. 2015;64:127–36.

1247 81. Uyeda JC, Zenil-Ferguson R, Pennell MW. Rethinking phylogenetic comparative methods. Syst
1248 Biol. 2018;67:1091–109.

1249 82. Kamimura Y. Copulation anatomy of *Drosophila melanogaster* (Diptera: Drosophilidae): wound-
1250 making organs and their possible roles. Zoomorphology. 2010;129:163–74.

1251 83. Schärer L. Tests of sex allocation theory in simultaneously hermaphroditic animals. Evolution.
1252 2009;63:1377–405.

1253 84. Ladurner P, Schärer L, Salvenmoser W, Rieger RM. A new model organism among the lower
1254 Bilateria and the use of digital microscopy in taxonomy of meiobenthic Platyhelminthes:

1255 *Macrostomum lignano*, n. sp. (Rhabditophora, Macrostomorpha). J Zool Syst Evol Res.
1256 2005;43:114–26.

1257 85. Janicke T, Marie-Orleach L, De Mulder K, Berezikov E, Ladurner P, Vizoso DB, et al. Sex
1258 allocation adjustment to mating group size in a simultaneous hermaphrodite. Evolution.
1259 2013;67:3233–42.

1260 86. Marie-Orleach L, Janicke T, Vizoso DB, David P, Schärer L. Quantifying episodes of sexual
1261 selection: insights from a transparent worm with fluorescent sperm. Evolution. 2016;70:314–28.

1262 87. Miller GT, Pitnick S. Sperm-female coevolution in *Drosophila*. Science. 2002;298:1230–3.

1263 88. Lüpold S, Manier MK, Berben KS, Smith KJ, Daley BD, Buckley SH, et al. How multivariate
1264 ejaculate traits determine competitive fertilization success in *Drosophila melanogaster*. Curr Biol.
1265 2012;22:1667–72.

1266 89. Manier MK, Lüpold S, Belote JM, Starmer WT, Berben KS, Ala-Honkola O, et al. Postcopulatory
1267 sexual selection generates speciation phenotypes in *Drosophila*. Curr Biol. 2013;23:1853–62.

1268 90. Parker GA, Immler S, Pitnick S, Birkhead TR. Sperm competition games: Sperm size (mass) and
1269 number under raffle and displacement, and the evolution of P2. J Theor Biol. 2010;264:1003–23.

1270 91. Willems M, Leroux F, Claeys M, Boone M, Mouton S, Artois T, et al. Ontogeny of the complex
1271 sperm in the macrostomid flatworm *Macrostomum lignano* (Macrostomorpha, Rhabditophora). J
1272 Morphol. 2009;270:162–74.

1273 92. Birkhead TR, Hosken DJ, Pitnick S. Sperm Biology. 2009.

1274 93. Reinhardt K, Dobler R, Abbott J. An Ecology of Sperm: Sperm Diversification by Natural
1275 Selection. Annu Rev Ecol Evol Syst. 2015;46:435–59.

1276 94. Hoogstraal H, Usinger RL. Monograph of Cimicidae (Hemiptera-Heteroptera). J Parasitol.
1277 1967;53:222.

1278 95. Schärer L, Ladurner P, Seifarth C, Salvenmoser W, Zaubzer J. Tracking sperm of a donor in a
1279 recipient: an immunocytochemical approach. Anim Biol. 2007;57:121–36.

1280 96. Giannakara A, Schärer L, Ramm SA. Sperm competition-induced plasticity in the speed of
1281 spermatogenesis. BMC Evol Biol. 2016;16. doi:10.1186/s12862-016-0629-9.

1282 97. Giannakara A, Ramm SA. Self-fertilization, sex allocation and spermatogenesis kinetics in the
1283 hypodermically inseminating flatworm *Macrostomum pusillum*. J Exp Biol. 2017;220:1568–77.

1284 98. Pitnick S, Markow TA, Spicer GS. Delayed male maturity is a cost of producing large sperm in
1285 Drosophila. Proc Natl Acad Sci. 1995;92:10614–8.

1286 99. Pitnick S. Investment in Testes and the Cost of Making Long Sperm in Drosophila. Am Nat.
1287 1996;148:57–80.

1288 100. Rohde K, Faubel A. Spermatogenesis of *Macrostomum pusillum* (Platyhelminthes,
1289 Macrostomida). Invertebr Reprod Dev. 1997;32:209–15.

1290 101. Rohde K, Watson N. Ultrastructure of spermatogenesis and sperm of *Macrostomum tuba*. J
1291 Submicrosc Cytol Pathol. 1991;23:23–32.

1292 102. Faubel A, Blome D, Cannon LRG. Sandy beach meiofauna of eastern Australia (southern
1293 Queensland and New South Wales). I. Introduction and macrostomida (Platyhelminthes). Invertebr
1294 Syst. 1994;8:899–1007.

1295 103. Anthes N, Schulenburg H, Michiels NK. Evolutionary links between reproductive morphology,
1296 ecology and mating behavior in opisthobranch gastropods. Evolution. 2008;62:900–16.

1297 104. Brennan PLR, Prum RO, McCracken KG, Sorenson MD, Wilson RE, Birkhead TR. Coevolution
1298 of Male and Female Genital Morphology in Waterfowl. PLOS ONE. 2007;2:e418.

1299 105. Arnqvist G, Rowe L. Correlated evolution of male and female morphologles in water striders.
1300 Evol Int J Org Evol. 2002;56:936–47.

1301 106. McPeek MA, Shen L, Farid H. The Correlated Evolution of Three-Dimensional Reproductive
1302 Structures Between Male and Female Damselflies. Evolution. 2009;63:73–83.

1303 107. Simmons LW, Fitzpatrick JL. Female genitalia can evolve more rapidly and divergently than
1304 male genitalia. Nat Commun. 2019;10:1312.

1305 108. Eberhard W. Female control: sexual selection by cryptic female choice. Princeton: Princeton
1306 University Press; 1996.
1307 http://www.degruyter.com/view/books/9780691207209/9780691207209/9780691207209.xml.
1308 Accessed 16 May 2020.

1309 109. Arnqvist G, Edvardsson M, Friberg U, Nilsson T. Sexual conflict promotes speciation in insects.
1310 Proc Natl Acad Sci. 2000;97:10460–4.

1311 110. Ritchie MG. Sexual Selection and Speciation. Annu Rev Ecol Evol Syst. 2007;38:79–102.

1312 111. Janicke T, Schärer L. Sperm competition affects sex allocation but not sperm morphology in a
1313 flatworm. Behav Ecol Sociobiol. 2010;64:1367–75.

1314 112. Tyler S, Schilling S, Hooge M, Bush L F. Turbellarian taxonomic database. 2006.

1315 113. Chambrier A, Zehnder M, Vaucher C, Mariaux J. The evolution of the Proteocephalidea
1316 (Platyhelminthes, Eucestoda) based on an enlarged molecular phylogeny, with comments on their
1317 uterine development. Syst Parasitol. 2004;57:159–71.

1318 114. Chambrier A de, Waeschenbach A, Fisseha M, Scholz T, Mariaux J. A large 28S rDNA-based
1319 phylogeny confirms the limitations of established morphological characters for classification of
1320 proteocephalidean tapeworms (Platyhelminthes, Cestoda). ZooKeys. 2015;500:25–59.

1321 115. Scarpa F, Cossu P, Sanna D, Lai T, Norenburg JL, Curini-Galletti M, et al. An 18S and 28S-
1322 based clock calibration for marine Proseriata (Platyhelminthes). J Exp Mar Biol Ecol. 2015;463:22–
1323 31.

1324 116. Templeton AR, Crandall KA, Sing CF. A cladistic analysis of phenotypic associations with
1325 haplotypes inferred from restriction endonuclease mapping and DNA sequence data. III. Cladogram
1326 estimation. Genetics. 1992;132:619–33.

1327 117. Clement M, Posada D, Crandall KA. TCS: a computer program to estimate gene genealogies.
1328 Mol Ecol. 2000;9:1657–9.

1329 118. Vanhove MPM, Tessens B, Schoelinck C, Jondelius U, Littlewood DTJ, Artois T, et al.
1330 Problematic barcoding in flatworms: A case-study on monogeneans and rhabdocoels
1331 (Platyhelminthes). ZooKeys. 2013;:355–79.

1332 119. Simmons MP, Müller K, Norton AP. The relative performance of indel-coding methods in
1333 simulations. Mol Phylogenet Evol. 2007;44:724–40.

1334 120. Brand JN, Wiberg RAW, Pjeta R, Bertemes P, Beisel C, Ladurner P, et al. RNA-Seq of three
1335 free-living flatworm species suggests rapid evolution of reproduction-related genes. BMC Genomics.
1336 2020;21:462.

1337 121. Wudarski J, Simanov D, Ustyantsev K, de Mulder K, Grelling M, Grudniewska M, et al.
1338 Efficient transgenesis and annotated genome sequence of the regenerative flatworm model
1339 *Macrostomum lignano*. Nat Commun. 2017;8:2120.

1340 122. Grudniewska M, Mouton S, Grelling M, Wolters AHG, Kuipers J, Giepmans BNG, et al. A
1341 novel flatworm-specific gene implicated in reproduction in *Macrostomum lignano*. Sci Rep.
1342 2018;8:3192.

1343 123. Smith-Unna R, Boursnell C, Patro R, Hibberd JM, Kelly S. TransRate: reference-free quality
1344 assessment of de novo transcriptome assemblies. Genome Res. 2016;26:1134–44.

1345 124. Waterhouse RM, Seppey M, Simão FA, Manni M, Ioannidis P, Klioutchnikov G, et al. BUSCO
1346 applications from quality assessments to gene prediction and phylogenomics. Mol Biol Evol. 2017.
1347 https://academic.oup.com/mbe/advance-article/doi/10.1093/molbev/msx319/4705839. Accessed 8
1348 Dec 2017.

1349 125. Zaharia M, Bolosky WJ, Curtis K, Fox A, Patterson D, Shenker S, et al. Faster and more accurate
1350 sequence alignment with SNAP. ArXiv Prepr ArXiv11115572. 2011.

1351 126. Haas BJ, Papanicolaou A, Yassour M, Grabherr M, Blood PD, Bowden J, et al. *De novo*
1352 transcript sequence reconstruction from RNA-seq using the Trinity platform for reference generation
1353 and analysis. Nat Protoc. 2013;8:1494–512.

1354 127. Fu L, Niu B, Zhu Z, Wu S, Li W. CD-HIT: accelerated for clustering the next-generation
1355 sequencing data. Bioinformatics. 2012;28:3150–2.

1356 128. Emms DM, Kelly S. OrthoFinder: solving fundamental biases in whole genome comparisons
1357 dramatically improves orthogroup inference accuracy. Genome Biol. 2015;16:157.

1358 129. Yang Y, Smith SA. Orthology inference in nonmodel organisms using transcriptomes and low-
1359 coverage genomes: improving accuracy and matrix occupancy for phylogenomics. Mol Biol Evol.
1360 2014;31:3081–92.

1361 130. Nakamura T, Yamada KD, Tomii K, Katoh K, Hancock J. Parallelization of MAFFT for large-
1362 scale multiple sequence alignments. Bioinformatics. 2018;34:2490–2.

1363 131. Kalyaanamoorthy S, Minh BQ, Wong TKF, Haeseler A von, Jermiin LS. ModelFinder: fast
1364 model selection for accurate phylogenetic estimates. Nat Methods. 2017;14:587–9.

1365 132. Wu M, Chatterji S, Eisen JA. Accounting for alignment uncertainty in phylogenomics. PLOS
1366 ONE. 2012;7:e30288.

1367 133. Roure B, Baurain D, Philippe H. Impact of missing data on phylogenies inferred from empirical
1368 phylogenomic data sets. Mol Biol Evol. 2013;30:197–214.

1369 134. Tan G, Muffato M, Ledergerber C, Herrero J, Goldman N, Gil M, et al. Current methods for
1370 automated filtering of multiple sequence alignments frequently worsen single-gene phylogenetic
1371 inference. Syst Biol. 2015;64:778–91.

1372 135. Wang H-C, Minh BQ, Susko E, Roger AJ. Modeling site heterogeneity with posterior mean site
1373 frequency profiles accelerates accurate phylogenomic estimation. Syst Biol. 2018;67:216–35.

1374 136. Plummer M, Best N, Cowles K, Vines K. CODA: convergence diagnosis and output analysis
1375 for MCMC. R News. 2006;6:7–11.

1376 137. Capella-Gutierrez S, Silla-Martinez JM, Gabaldon T. trimAl: a tool for automated alignment
1377 trimming in large-scale phylogenetic analyses. Bioinformatics. 2009;25:1972–3.

1378 138. Sanderson MJ. Estimating absolute rates of molecular evolution and divergence times: A
1379 penalized likelihood approach. Mol Biol Evol. 2002;19:101–9.

1380 139. Smith SA, O'Meara BC. treePL: divergence time estimation using penalized likelihood for large
1381 phylogenies. Bioinformatics. 2012;28:2689–90.

1382 140. Bollback JP. SIMMAP: Stochastic character mapping of discrete traits on phylogenies. BMC
1383 Bioinformatics. 2006;7:88.

1384 141. Revell LJ. phytools: an R package for phylogenetic comparative biology (and other things):
1385 phytools: R package. Methods Ecol Evol. 2012;3:217–23.

1386 142. Pagel M. Detecting correlated evolution on phylogenies: a general method for the comparative
1387 analysis of discrete characters. Proc R Soc Lond B. 1994;255:37–45.

1388 143. Revell LJ. Size-correction and principal components for interspecific comparative studies.
1389 Evolution. 2009;63:3258–68.

1390 144. Peres-Neto PR, Jackson DA, Somers KM. Giving meaningful interpretation to ordination axes:
1391 assessing loading significance in principal component analysis. Ecology. 2003;84:2347–63.

1392 145. Ives AR. R^2s for Correlated Data: Phylogenetic Models, LMMs, and GLMMs. Syst Biol.
1393 2019;68:234–51.

1394 146. Ives A, Li D. rr2: An R package to calculate R^2s for regression models. J Open Source Softw.
1395 2018;3:1028.

1396 147. Wang A-T. Three new species of the genus *Macrostomum* from China (Platyhelminthes,
1397 Macrostomida, Macrostomidae). Acta Zootaxonomica Sin. 2005;30:714–20.

1398 148. Sun T, Zhang L, Wang A-T, Zhang Y. Three new species of freshwater *Macrostomum*
1399 (Platyhelminthes, Macrostomida) from southern China. Zootaxa. 2015;4012:120–34.

1400 149. Lin Y, Zhou W, Xiao P, Zheng Y, Lu J, Li J, et al. Two new species of freshwater *Macrostomum*
1401 (Rhabditophora: Macrostomorpha) found in China. Zootaxa. 2017;4329:267.

150. Lin Y-T, Feng W-T, Xin F, Zhang L, Zhang Y, Wang A-T. Two new species and the molecular phylogeny of eight species of *Macrostomum* (Platyhelminthes: Macrostomorpha) from southern China. Zootaxa. 2017;4337:423.

151. Wang L, Xin F, Fang C-Y, Zhang Y, Wang A-T. Two new brackish-water species of *Macrostomum* (Platyhelminthes, Macrostomida) from mangrove wetland in southern China. Zootaxa. 2017;4276:107.

Figures

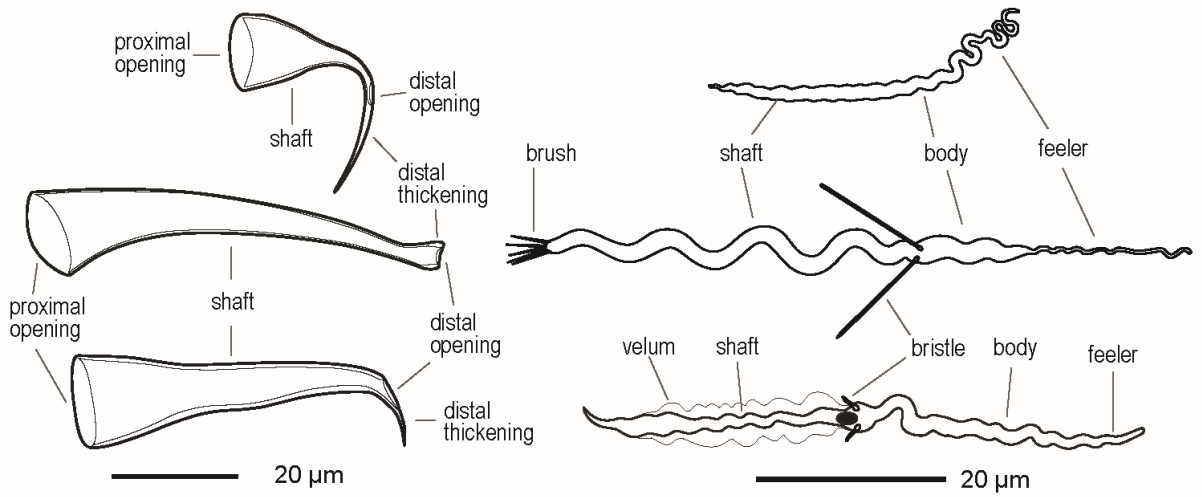

Fig 1. Representative drawings of the morphology of the stylet (male intromittent organ) (left) and the sperm (right) of three *Macrostomum* species.
Top: *M.* sp. 92, a hypodermically mating species from the hypodermic clade, with a typical needle-like stylet and a simple sperm morphology. Middle: The well-studied model organism *M. lignano* with the typical morphology for reciprocally mating species, showing a stylet with blunt distal thickenings and a complex sperm with an anterior feeler, two stiff lateral bristles, and a terminal brush. Bottom: *M.* sp. 9 representing one of the convergent origins of hypodermic insemination in the reciprocal clade, showing a stylet with a highly asymmetric and sharp distal thickening and sperm with reduced sperm bristles, no brush, but a thin velum along the shaft. Note that, given the striking diversity across the *Macrostomum* genus, it is not possible to clearly delimit all the sperm traits originally defined in *M. lignano* in some of the species.

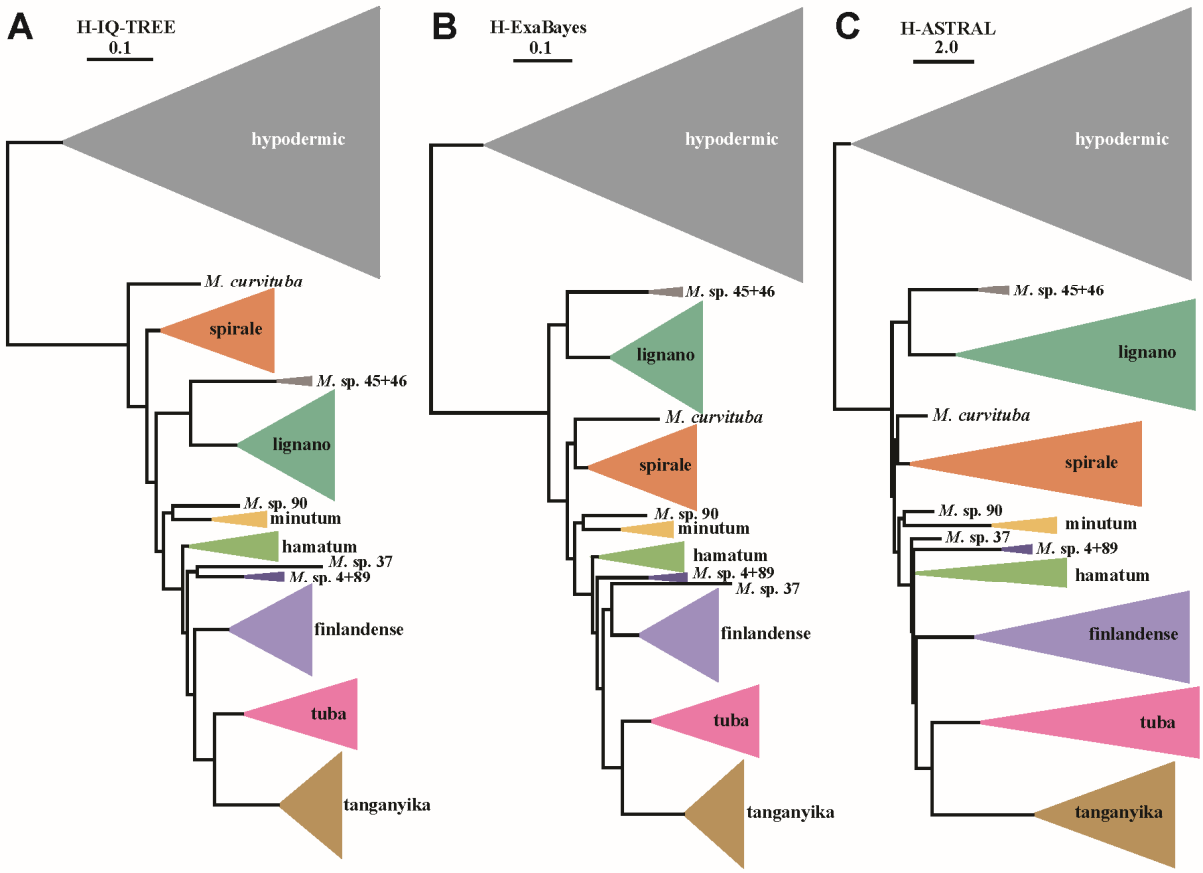

Fig 2. Simplified phylogenies of the genus *Macrostomum*.
Consistently recovered clades are collapsed into named triangles, with the height of the base proportional to the number of species, and single species names preceded by the genus abbreviation (in italics). Not shown here is the variable placement of *M.* sp. 39 within the hypodermic clade (see Figure S1). (A) Maximum-likelihood phylogeny (H-IQ-TREE) (B) Bayesian phylogeny (H-ExaBayes). (C) Summary method phylogeny (H-ASTRAL). Branch length represents substitutions per site in A & B and coalescent units in C. Support values for these groupings are generally high (for details see **Fig S1**).

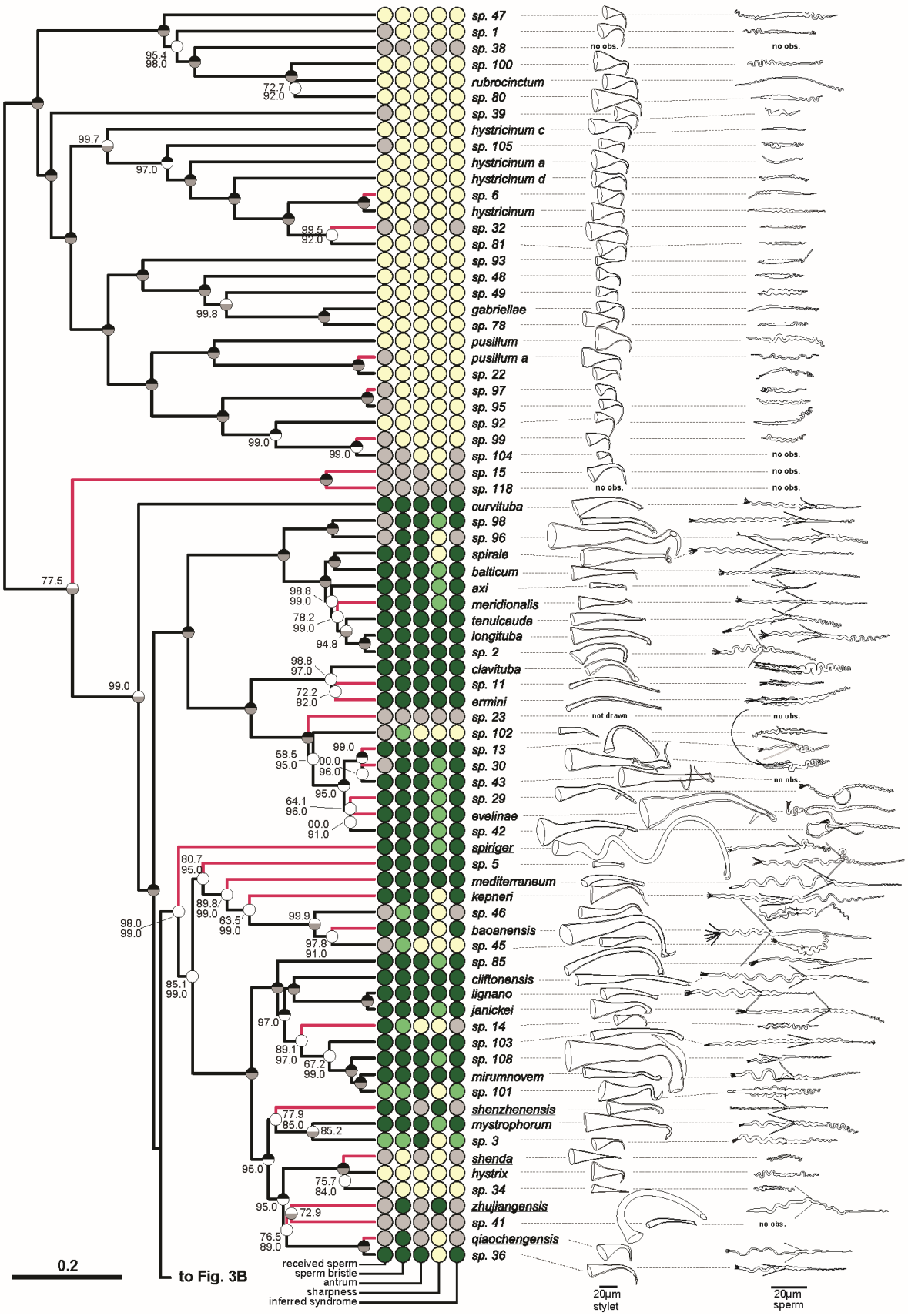
sp. 47
sp. 1
sp. 38
sp. 100
rubrocinctum
sp. 80
sp. 39
hystricinum c
sp. 105
hystricinum a
hystricinum d
sp. 6
hystricinum
sp. 32
sp. 81
sp. 93
sp. 48
sp. 49
gabriellae
sp. 78
pusillum
pusillum a
sp. 22
sp. 97
sp. 95
sp. 92
sp. 99
sp. 104
sp. 15
sp. 118
curvituba
sp. 98
sp. 96
spirale
balticum
axi
meridionalis
tenuicauda
longituba
sp. 2
clavituba
sp. 11
ermini
sp. 23
sp. 102
sp. 13
sp. 30
sp. 43
sp. 29
evelinae
sp. 42
spiriger
sp. 5
mediterraneum
kepneri
sp. 46
baoanensis
sp. 45
sp. 85
cliftonensis
lignano
janickei
sp. 14
sp. 103
sp. 108
mirumnovem
sp. 101
shenzhenensis
mystrophorum
sp. 3
shenda
hystrix
sp. 34
zhujiangensis
sp. 41
qiaochengensis
sp. 36
no obs.
not drawn
0.2
to Fig. 3B
received sperm
sperm bristle
antrum
sharpness
inferred syndrome
20µm
stylet
20µm
sperm

1430

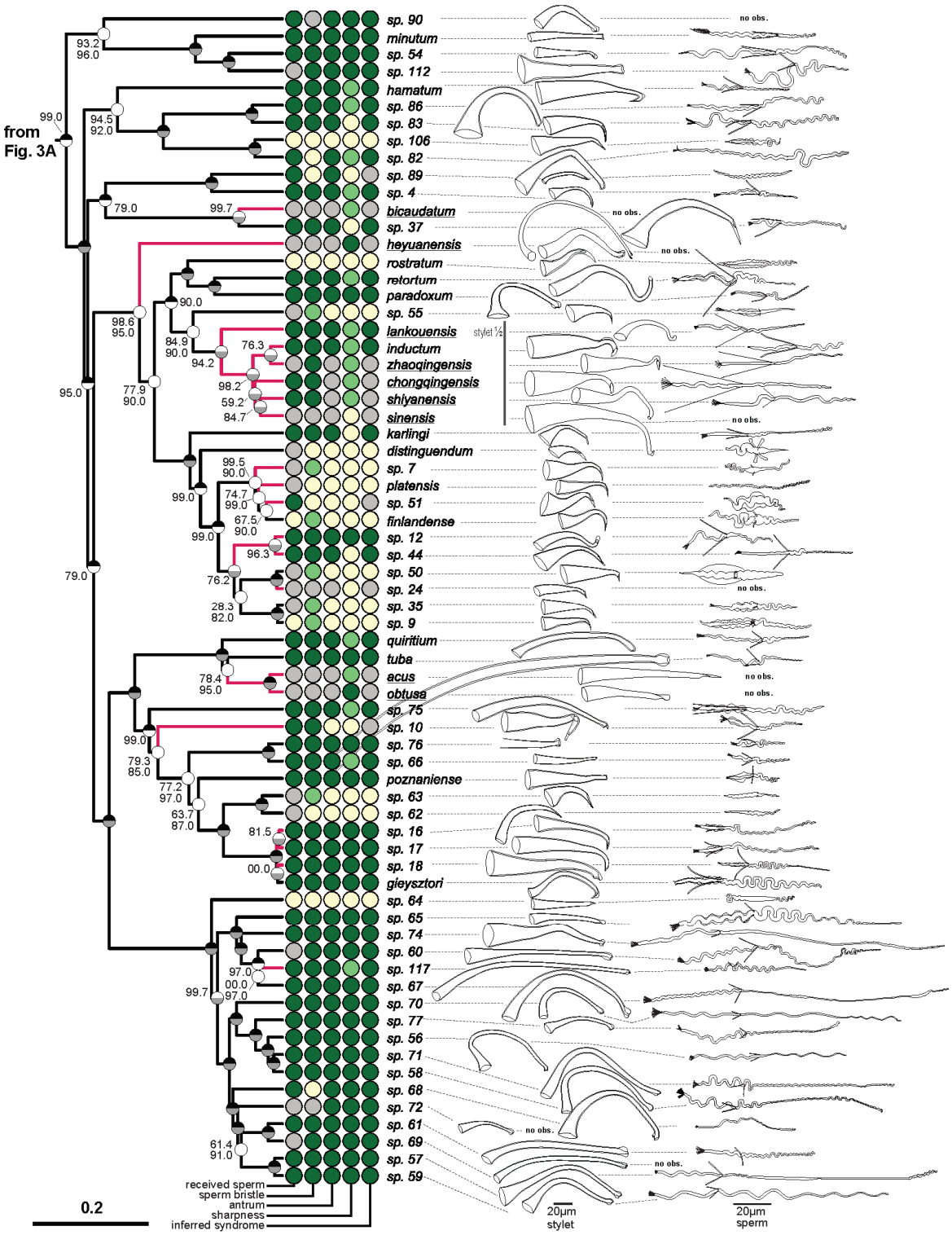
from Fig. 3A
sp. 90
minutum
sp. 54
sp. 112
hamatum
sp. 86
sp. 83
sp. 106
sp. 82
sp. 89
sp. 4
bicaudatum
sp. 37
heyuanensis
rostratum
retortum
paradoxum
sp. 55
lankouensis
inductum
zhaoqingensis
chongqingensis
shiyanensis
sinensis
karlingi
distinguendum
sp. 7
platensis
sp. 51
finlandense
sp. 12
sp. 44
sp. 50
sp. 24
sp. 35
sp. 9
quiritium
tuba
acus
obtusa
sp. 75
sp. 10
sp. 76
sp. 66
poznaniense
sp. 63
sp. 62
sp. 16
sp. 17
sp. 18
gieysztori
sp. 64
sp. 65
sp. 74
sp. 60
sp. 117
sp. 67
sp. 70
sp. 77
sp. 56
sp. 71
sp. 58
sp. 68
sp. 72
sp. 61
sp. 69
sp. 57
sp. 59
no obs.
stylet ½
received sperm
sperm bristle
antrum
sharpness
inferred syndrome
0.2
20µm stylet
20µm sperm

1431

Fig 3. Phylogeny of the genus *Macrostomum*, showing the striking diversity in stylet and sperm morphology across the genus.
The ultrametric phylogeny (C-IQ-TREE) includes all 145 studied species (with 77 species depicted in Fig 3A and 68 species in Fig 3B). Branch supports are ultrafast bootstraps (top, black if 100) and approximate likelihood ratio tests (bottom, grey if 100). Species without available transcriptomes that were added based on a *28S rRNA* fragment are indicated with red branches. Columns indicate the states of five reproductive traits from light to dark (i.e. yellow, light green and dark green for trinary states; or yellow and dark green for binary states; grey indicates missing data): received sperm location (hypodermic, both, in antrum), sperm bristle state (absent, reduced, present), antrum state (simple, thickened), sharpness of stylet (sharp, neutral, blunt), inferred mating syndrome (hypodermic, intermediate, reciprocal). Stylet and sperm are drawn based on our live observations, except for species with underlined names, which were redrawn based on the species description (*M. acus*, *M. obtusa* and *M. sinensis* from Wang 2005; *M. heyuanensis* and *M. bicaudatum* from Sun et al. 2015; *M. chongqingensis* and *M. zhaoqingensis* from Lin et al. 2017a; *M. shiyanensis* and *M. lankouensis* from Lin et al. 2017b; *M. shenzhenensis* and *M. qiaochengensis* from Wang et al. 2017; and *M. spiriger* and *M. shenda* from Xin et al. 2019). The stylet of *M*. sp. 15 is not drawn to scale, the stylets of some species are drawn at half size (stylet ½), and the stylet of *M*. sp. 23 is not drawn since it was incomplete (specimen ID MTP LS 913). Unobserved structures are marked as no observation (no obs.).

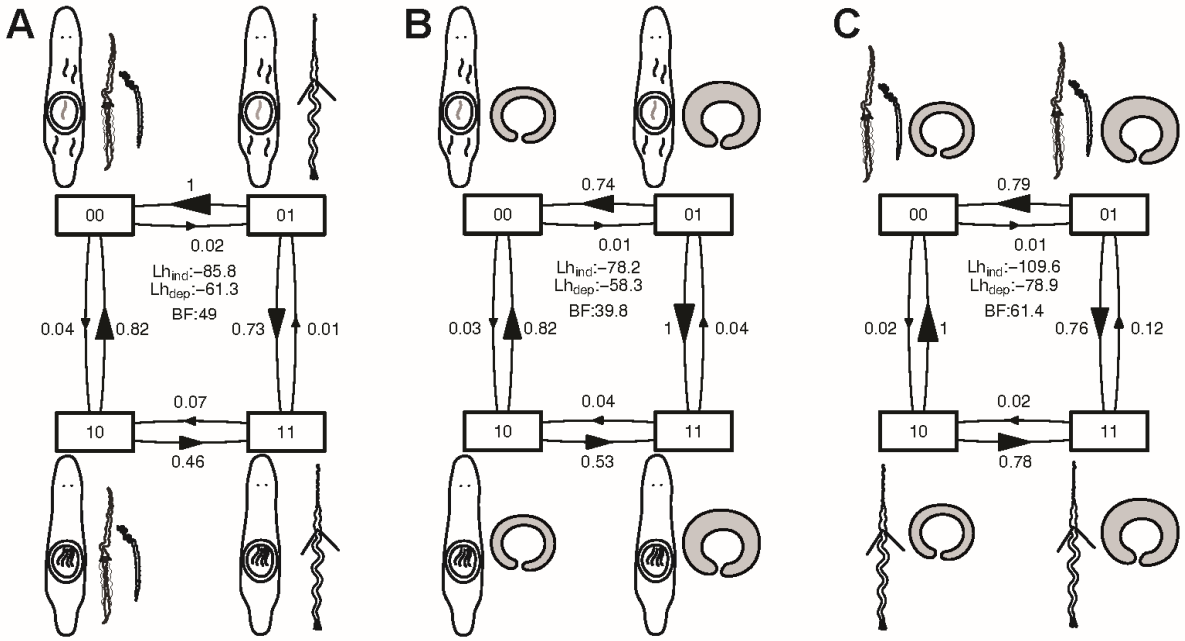

Fig 4. Results of correlated evolution analysis between (A) received sperm location and sperm bristle state, (B) received sperm location and antrum state, and (C) sperm bristle state and antrum state.
Shown are transition matrices for the dependent model from BayesTraits analysis, which was always preferred over the independent model. Transition rates are scaled so that the largest is unity (and arrow sizes are proportional). Also given are the likelihoods of the independent (Lh_{ind}) and dependent (Lh_{dep}) models, and the resulting BayesFactors (BF). An exponential prior and the C-IQ-TREE phylogeny was used for the results shown here. See SI Correlated evolution for runs with other priors (uniform and reversible-jump hyperprior) and other phylogenies (H-IQ-TREE and H-ExaBayes), which show qualitatively similar results.

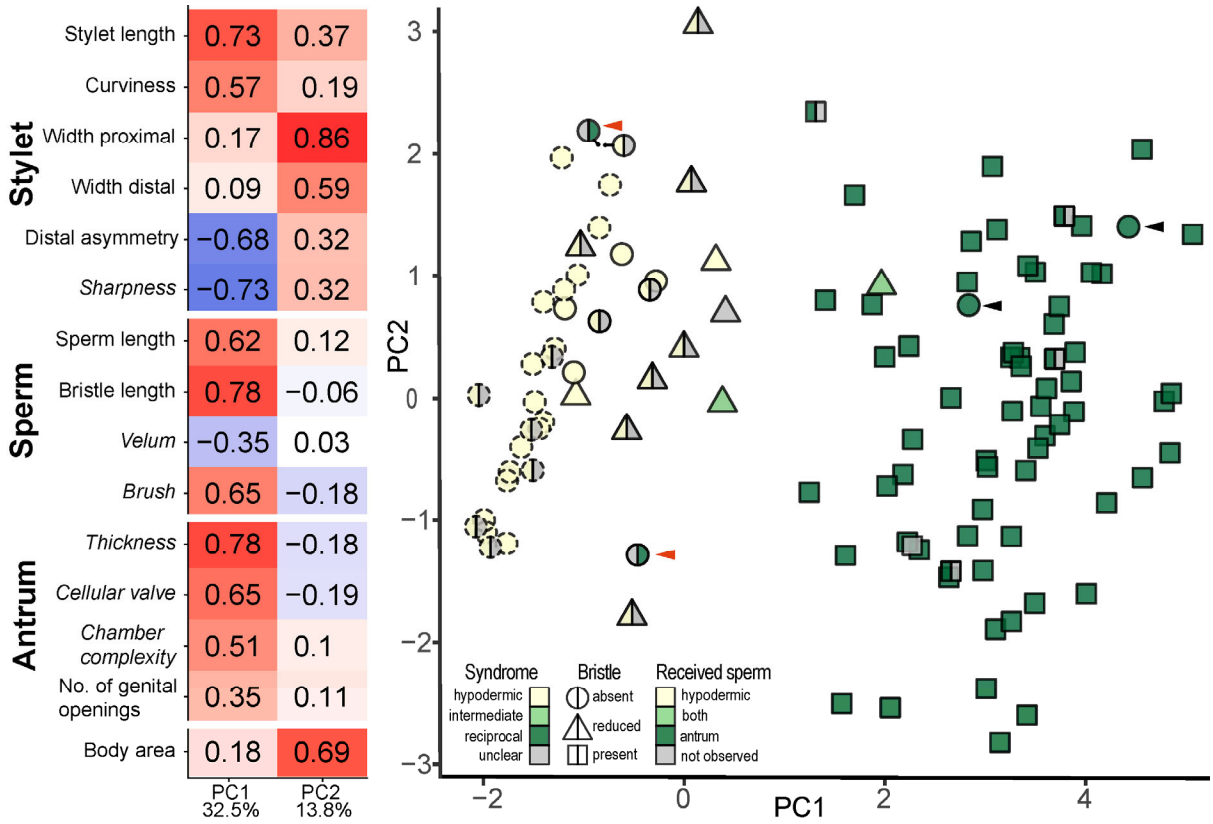

Fig 5. Results of a phylogenetically corrected principal component analysis of the measured quantitative and categorical (italics) reproductive traits.
Left: Loadings of PC1 and PC2, with the percentage of variance explained at the bottom. Right: 2D morphospace defined by PC1 and PC2. As indicated by the legend, the shape represents the sperm bristle state, while the colours represent the inferred mating syndrome (left side) and the received sperm location (right side). Species from the hypodermic clade are outlined with stippled lines. Red arrowheads indicate two species (*Macrostomum* sp. 51 and *M*. sp. 89) that cluster closely with species assigned to the hypodermic mating syndrome, but in which we observed received sperm in the antrum. Black arrowheads indicate two species (*M*. sp. 68 and *M*. sp. 82) assigned to the reciprocal syndrome, which have no discernible sperm bristles (see also Fig 6). The phylogenetic relationships of these species are represented as a phylomorphospace animation in Fig S4. Results shown here based on C-IQ-TREE, while detailed results including analyses with other phylogenies (H-IQ-TREE and H-ExaBayes) are in Tab S5**Fig S3**.

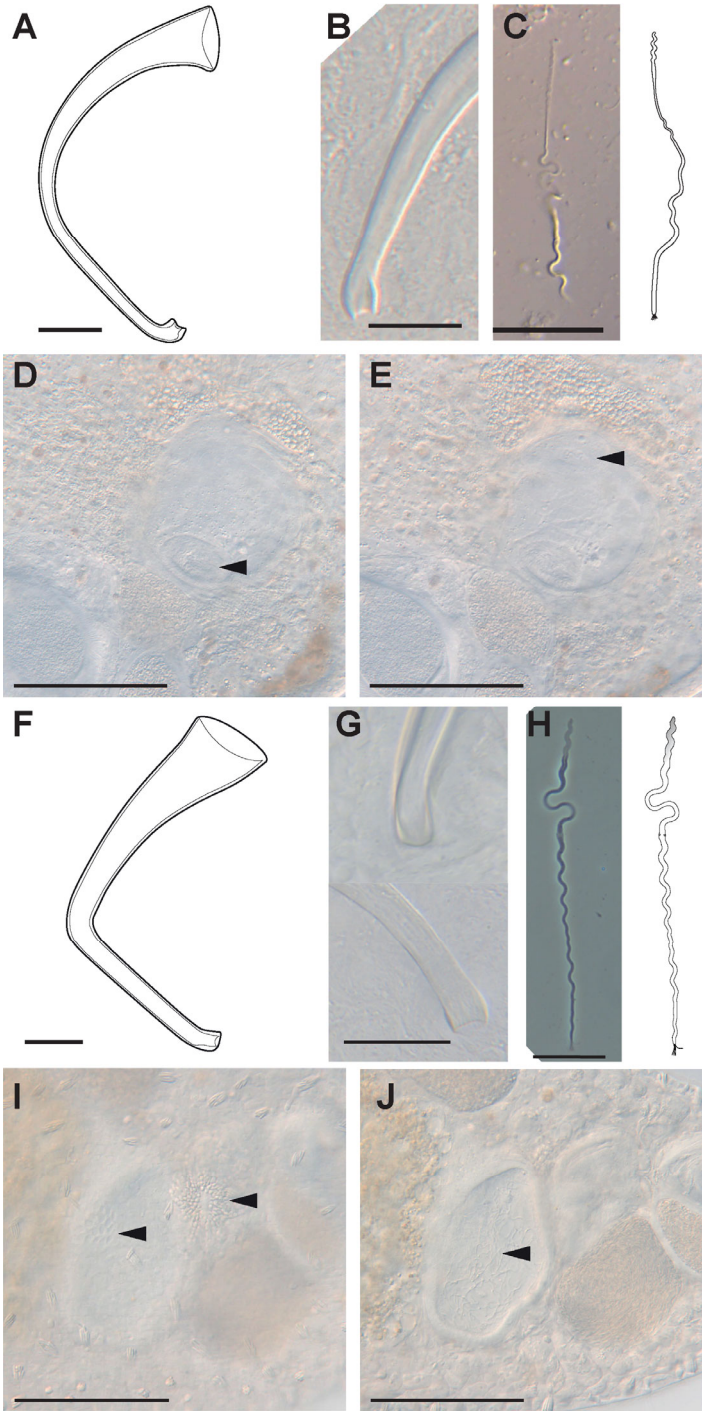

Fig 6. Details on the reproductive morphology of *Macrostomum* sp. 68 (A-E) and *M.* sp. 82 (F-J). *M.* sp. 68 (A) Stylet drawing showing the blunt distal thickenings; (B) distal stylet tip in a smash preparation (specimen ID MTP LS 2611). (C) Sperm image (MTP LS 2686) and drawing showing what seems to be a long feeler, but no apparent sperm bristles. (D-E). Details of the antrum (MTP LS 2562) indicating the muscular connection between the female genital opening and the antrum (arrowhead in D) and the anterior second chamber containing at least one received sperm (arrowhead in E). *M.* sp. 82 (F) Drawing of the stylet showing the slight blunt distal thickenings. (G) Distal stylet tip *in situ* (top, MTP LS 2845) and in a smash preparation (bottom, MTP LS 2846). (H) Sperm image (MTP LS 2877) and drawing indicating the modified anterior part of the sperm (shaded grey) and a less dense area approximately 1/3 along the sperm, which could be a vestigial bristle anchor location (arrowhead). (I-J) Details of the antrum (MTP LS 2848) indicating the anterior genital opening, the bursa pore (I, left arrowhead) next to the posterior genital opening, the gonopore (I, right arrowhead), both connecting into a large chamber containing many received sperm (J, arrowhead). Scale bars represent 100 µm in the antrum images and 20 µm otherwise.

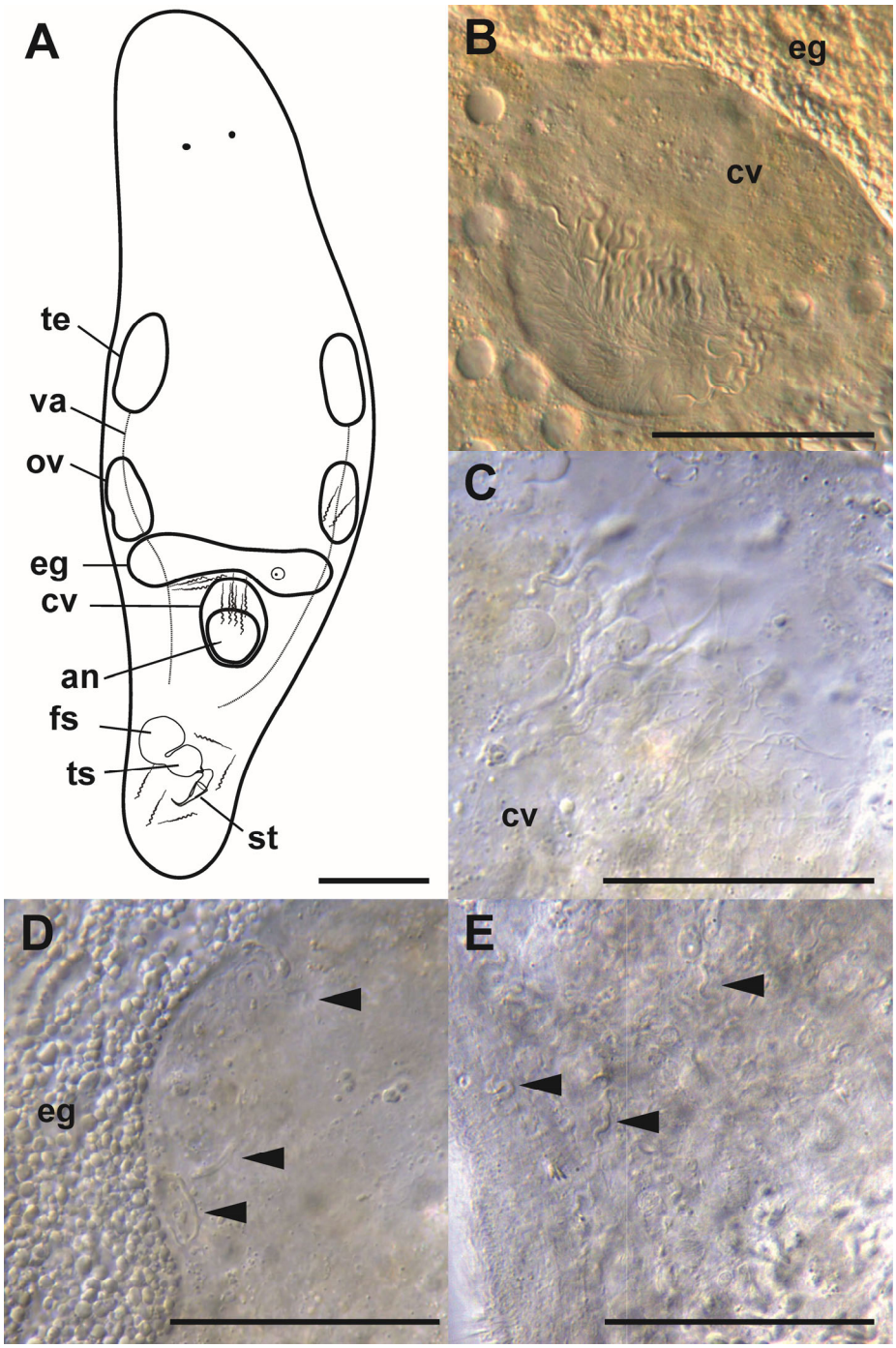

Fig 7. Detailed observations of received sperm location in *Macrostomum* sp. 3.
(A) Drawing of the sexual organs (te: testis, vd: vas deferens, ov: ovary, eg: developing egg, cv: cellular valve, an: antrum, fs: false seminal vesicle, ts: true seminal vesicle, st: stylet), with sperm drawn at locations where they were observed. (B-E) show sperm *in situ*. (B) sperm in the antrum (specimen ID MTP LS 3286) embedded in the cellular valve (anterior); (C) sperm in cellular valve with loose tissue (MTP LS 3314); (D) sperm close to developing egg (MTP LS 3314); (E) sperm close to the ovary (MTP LS 3317). Scale bars represent 100µm in (A) and 50 µm otherwise.

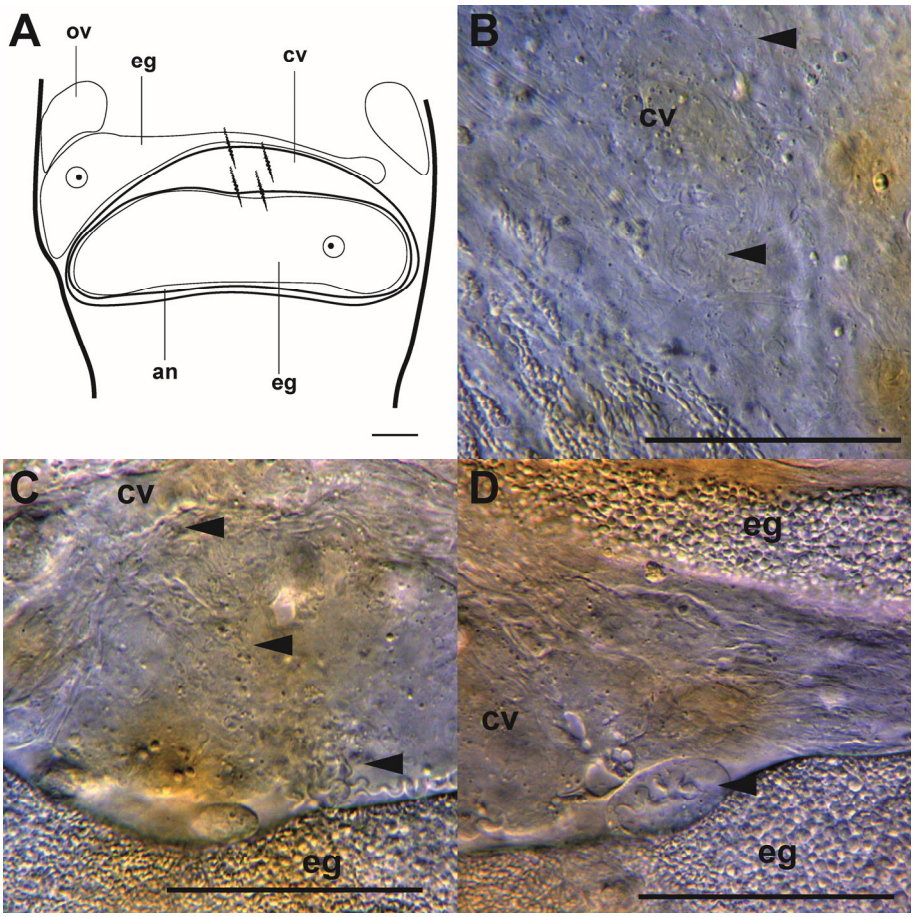

Fig 8. Detailed observations of received sperm location in *Macrostomum* sp. 101.
(A) Drawing of antrum region (ov: ovary, eg: developing egg, cv: cellular valve, an: antrum), with sperm drawn at locations where they were observed. (B-D) show sperm *in situ* with anterior on the top. (B) sperm (arrow) embedded in cellular valve (specimen ID MTP LS 3206); (C) sperm (arrow) in cellular valve and antrum (MTP LS 3127); (D) same specimen as C with dislodged sperm (arrow) surrounded by what appears to be cellular valve derived tissue. Scale bars represent 100µm in (A) and 50µm otherwise.

1500

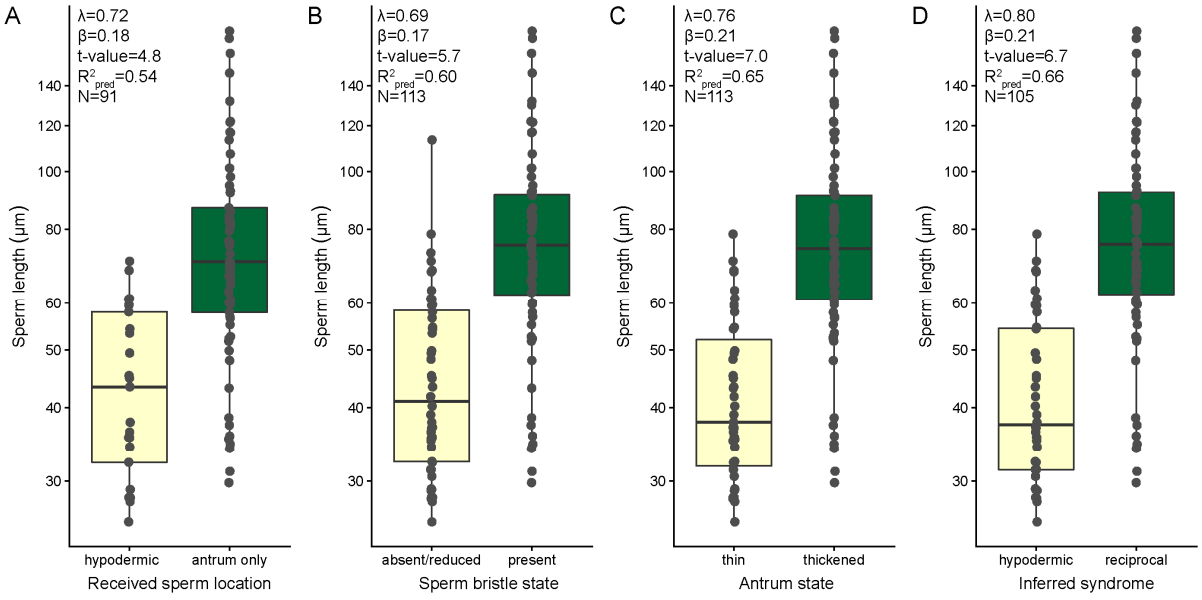

1501

1502 **Fig 9. Sperm length of species dependent on (A) sperm bristle state, (B) received sperm location (C) antrum state**
1503 **or (D) inferred mating syndrome.**
1504 Values are slightly jittered in the x direction, and the y-axis is on a log-scale. Within each panel the main results of
1505 PGLS analysis are given and in all tests the slopes were significant at $p < 0.001$. Detailed results including analyses with
1506 different phylogenies (H-IQ-TREE and H-ExaBayes) are given in Tab S6.

1507

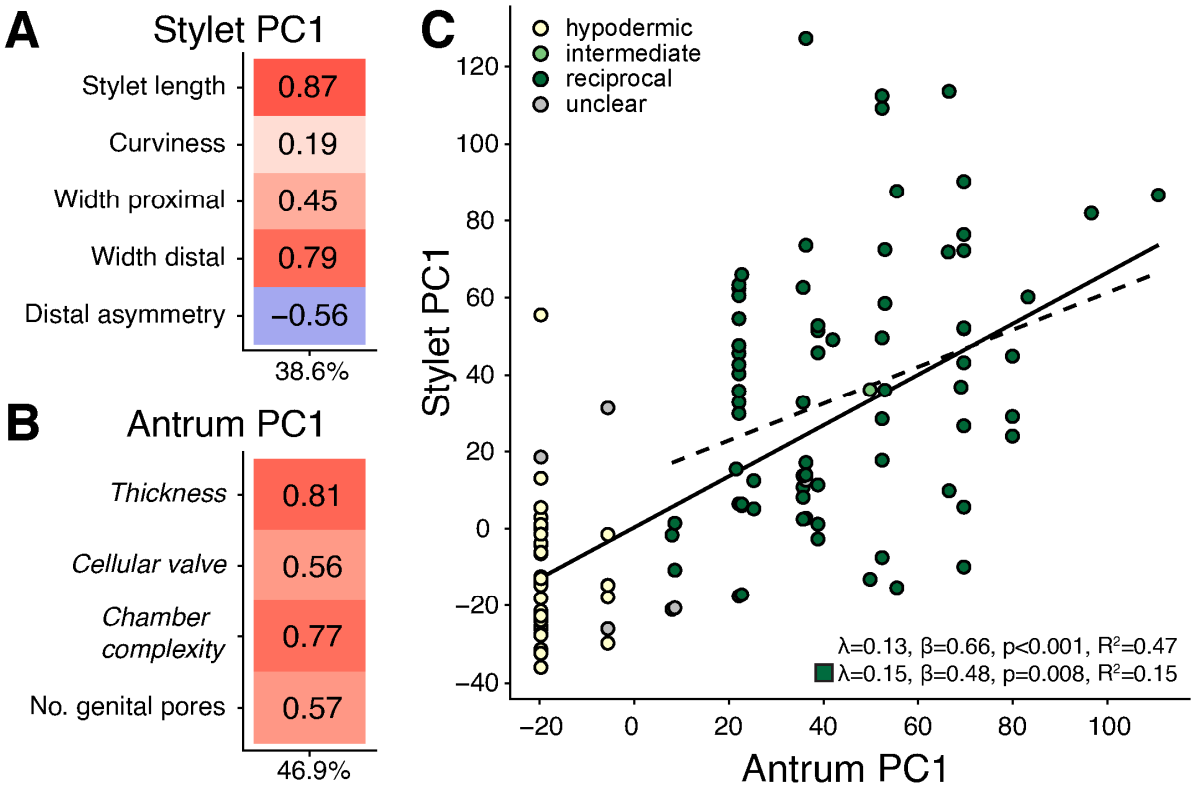

Fig 10. Phylogenetically corrected principal component analyses of stylet (A) and antrum (B) traits, and evidence for male-female coevolution (C).
Loadings of Stylet and Antrum PC1, with the percentage of variance explained at the bottom, of the stylet (A) and antrum (B) traits, respectively. Categorical reproductive traits are in italics. (C) Shows the results from PGLS regression between Stylet PC1 and Antrum PC1 from (A-B). Regression was performed across all species (solid line, upper statistics) and restricted to species of the reciprocal mating syndrome (dashed line, lower statistics). The inferred mating syndrome of species is indicated by the colour of the dots. Results based on C-IQ-TREE, detailed results including analysis with other phylogenies (H-IQ-TREE and H-ExaBayes) are in Tab S7.

1518 # Tables

1519

1520 **Tab 1. Summary of the taxonomic status of all the included *Macrostomum* species.**
1521 Species inferred based on single specimens (N=1) are listed separately.

Species in this study	N = 1	N > 1	Total
All	18	127	145
Described	5	46	51
Likely undescribed & immature	3	2	5
Likely undescribed, mature & no transcriptome	5	17	22
Likely undescribed, mature & transcriptome	5	62	67

1522

1523

1524 **Tab 2. Characteristics of the used protein alignments.**
1525 We used one alignment aimed at a high number of genes (L alignment) and one alignment aimed at high occupancy (H
1526 alignment). The alignments used were trimmed to only include regions with a high probability of being homologous
1527 using ZORRO, and the statistics are given for the alignments before and after trimming.

Alignment metrics	**L untrimmed**	**L**	**H untrimmed**	**H**
No. genes	8128	8128	385	385
No. amino acids AA	5,057,157	1,687,014	200,729	94,625
No. variable sites	3,263,955	1,157,689	135,887	74,175
No. parsimony informative sites	2,287,246	934,803	103,425	63,066
Missing data (%)	78.1	59.3	55.7	22.9

1528

1529

1530

1531 **Tab 3. Assignment of the inferred mating syndrome based on different reproductive traits.**
1532 Species were assigned to an inferred mating syndrome based on the location of received sperm in the body (antrum, in
1533 the antrum only; hypodermic, hypodermic only; both, in the antrum and hypodermic; NA, no observation), the sperm
1534 bristle state (absent, reduced or present), the antrum state (simple or thickened), and the shape of the distal thickening of
1535 the stylet (sharp or blunt). 26 species with either not enough (22 species) or contradictory (four species) information
1536 were not assigned to a syndrome. Note, that all 24 species with only hypodermic sperm had the same morphological
1537 states, but this was not a condition for their assignment (hence the brackets). Similarly, all 69 species assigned to the
1538 reciprocal mating syndrome had a thickened antrum, but this was not a condition for their assignment.

	Received sperm location				**Morphology**			
Syndrome	**Antrum**	**Hypodermic**	**Both**	**NA**	**Sperm bristle**	**Antrum**	**Stylet**	**N**
Hypodermic		24			(Reduced/absent)	(Simple)	(Sharp)	24
Hypodermic				18	Reduced/absent	Simple	Sharp	18
Intermediate			2		Reduced	Thickened	Sharp	2
Reciprocal	61			6	Any state	(Thickened)	Blunt	67
Reciprocal	8				Present	(Thickened)	Sharp	8
Unclear	7			19	Other combinations			26

1539

1540

1541

Tab 4. Ancestral state reconstructions of reproductive traits, including received sperm location, sperm bristle state, antrum state, and inferred mating syndrome.
A range of MK-models were compared based on their AIC weights (ER: equal rate, SYM: symmetrical rate, ORD-Dollo: ordered model without gains once the trait is in state 0, Dollo: model without gains, ORD: ordered model, ARD: all rates different). For each trait the model with the highest AICc weight is shown in bold type, but we estimated the number of transitions between the states using stochastic character mapping with 1000 posterior samples for all models with an AICc weight >0.15. Given are the average number of transitions and the 2.5% and 97.5% quantiles in brackets. Results are based on the C-IQ-TREE phylogeny. For the quantitatively similar results with the H-IQ-TREE and H-ExaBayes phylogenies see Table S4.

Reproductive trait	model	dfs	log lik	AICc	ΔAICc	AICc weight	$N_{Species}$	$N_{Changes}$	0 →1	1→0	1→2	2→1	0→2	2→0
Received sperm location 0: hypodermic only 1: hypodermic & in antrum 2: in antrum only	ER	1	-43.3	88.6	10.1	0.004								
	SYM	3	-40.9	88.1	9.6	0.005								
	ORD-Dollo	**3**	**-36.1**	**78.5**	**0**	**0.579**	**102**	**21.2 (16, 32)**	**-**	**8.0 (7, 13)**	**4.0 (0, 11)**	**9.3 (7, 13)**	**-**	**-**
	Dollo	4	-36.1	80.6	2.2	0.196	102	10.8 (9, 17)	-	0.8 (0, 4)	0.9 (0, 4)	2.6 (2, 5)	-	6.5 (4, 8)
	ORD	4	-36.1	80.6	2.2	0.196	102	23.4 (16, 38)	0.7 (0, 4)	8.4 (6, 13)	4.8 (0, 15)	9.6 (7, 15)	-	-
	ARD	6	-36.1	85.1	6.6	0.021								
Received sperm location 0: hypodermic 1: in antrum only	ER	1	-36.8	75.6	3.1	0.135								
	Dollo	**1**	**-35.2**	**72.5**	**0**	**0.638**	**102**	**9.3 (9, 11)**	**-**	**9.3 (9, 11)**				
	ARD	2	-35.2	74.5	2.1	0.227	102	9.9 (9, 14)	0.9 (0, 4)	9.0 (8, 12)				
Sperm bristle state 0: absent 1: reduced 2: present	ER	1	-82.9	167.8	27.2	0								
	SYM	3	-81.7	169.5	28.9	0								
	ORD-Dollo	**3**	**-67.2**	**140.6**	**0**	**0.578**	**131**	**36.3 (29, 48)**	**-**	**12.2 (11, 17)**	**6.7 (1, 16)**	**17.5 (14, 23)**	**-**	**-**
	Dollo	4	-67.2	142.7	2.1	0.2	131	29.3 (22, 41)	-	7.1 (3, 13)	5.3 (1, 13)	12.4 (8, 18)	-	4.6 (0, 8)
	ORD	4	-67.2	142.7	2.1	0.199	131	37.1 (29, 50)	0.8 (0, 5)	13.0 (10, 20)	6.0 (1, 14)	17.3 (14, 22)	-	-
	ARD	6	-67.2	147.1	6.5	0.023								
Sperm bristle state 0: absent or reduced 1: present	ER	1	-57.6	117.3	5.7	0.038								
	Dollo	**1**	**-54.8**	**111.6**	**0**	**0.635**	**131**	**18.8 (18, 22)**	**-**	**18.8 (18, 22)**				
	ARD	2	-54.4	112.9	1.3	0.327	131	20.5 (17, 29)	2.7 (0, 9)	17.8 (15, 23)				
Antrum state 0: simple 1: thickened	ER	1	-48.1	98.2	3.8	0.086								
	Dollo	**1**	**-46.2**	**94.4**	**0**	**0.577**	**127**	**14.7 (14, 17)**	**-**	**14.7 (14, 17)**				
	ARD	2	-45.7	95.5	1.1	0.337	127	15.2 (13, 21)	2.1 (0, 6)	13.1 (11, 16)				
Inferred mating syndrome 0: hypodermic 1: intermediate 2: reciprocal	ER	1	-59.3	120.6	16.2	0								
	SYM	3	-54.4	114.9	10.4	0.003								
	ORD-Dollo	**3**	**-49.1**	**104.5**	**0**	**0.578**	**119**	**34.1 (27, 47)**	**-**	**13.7 (12, 18)**	**7.1 (2, 16)**	**13.2 (10, 19)**	**-**	**-**
	Dollo	4	-49.1	106.6	2.1	0.199	119	16.6 (14, 25)	-	0.7 (0, 5)	1.1 (0, 6)	2.8 (2, 6)	-	11.9 (9, 15)
	ORD	4	-49.1	106.6	2.1	0.198	119	35.4 (27, 50)	1.0 (0, 5)	14.3 (11, 20)	7.2 (2, 16)	12.9 (9, 18)	-	-
	ARD	6	-49.1	111	6.5	0.022								
Inferred mating syndrome 0: hypodermic & intermediate 1: reciprocal	ER	1	-49.4	100.9	14.675	0.001								
	Dollo	**1**	**-42.1**	**86.26**	**0**	**0.997**	**119**	**14.7 (14, 17)**	**-**	**14.7 (14, 17)**				
	ARD	2	-47.3	98.68	12.421	0.002								

Supp. Figures

Fig S1. Phylogenetic trees inferred using various methods on the L and H alignments. Clades are coloured consistently between the panels, with six large species groups (hypodermic, dark grey; spirale, orange; lignano, dark green; finlandense, purple; tuba, pink; tanganyika, brown), two smaller species groups (minutum, yellow; hamatum, light green), and two consistent species pairs (*M*. sp. 45 + 46, light grey; *M*. sp. 4 + 89, dark blue). Transcriptomes that are placed differently between approaches are highlighted in red. Species assignments are given as a short six letter abbreviation in the name of the transcriptomes (three letters each for the genus and species, respectively). See

Tab S8 for details.

see the file Fig_S1.pdf

Fig S2. The two ASTRAL phylogenies with quartet support shown for each node.
(A) L-ASTRAL phylogeny, and (B) H-ASTRAL phylogeny. The pie charts at the nodes represent the quartet support for the three possible partitions at that node. Blue represents support for the species tree topology and orange and red represent support for one or the other of the two alternative partitions. Mostly blue pie charts indicate little conflict. This analysis indicates that there is substantial gene tree – species tree conflict throughout the genus.

see the file Fig_S2.pdf

Fig S3. Ancestral state reconstructions of reproductive traits using the C-IQ-TREE phylogeny.
The trait and type of scoring (binary/trinary) is indicated at the bottom of each panel. Stochastic character mapping is summarised with pie charts representing the proportion of stochastic maps with the respective state. Shown is the reconstruction of the best-fitting ordered model without losses. The average number of transitions is given in Tab 4, while the red stars and numbers indicate the lower-bound number of transitions that have likely occurred (i.e. separated by nodes with >95% posterior probability of the ancestral state), while acknowledging that the ancestral state of the genus is often unclear (hence the brackets). The colours indicate the six large species groups (hypodermic, dark grey; spirale, orange; lignano, dark green; finlandense, purple; tuba, pink; tanganyika, brown), two smaller species groups (minutum, yellow; hamatum, light green), and two consistent species pairs (*M*. sp. 45 + 46, light grey; *M*. sp. 4 + 89, dark blue).

see the file Fig_S3.pdf

Fig S4. Animation of the phylomorphospace represented by PC1 and PC2 of the species in the C-IQ-TREE phylogeny.
The animation initially shows a cladogram that then gradually transforms into the phylomorphospace, which was calculated using the phylomorphospace function in phytools.

see the file Fig_S4.gif

Supp. Tables

Tab S1. The number of specimens analysed per *Macrostomum* species for all the included quantitative traits.

see the file Tab_S1.xlsx

Tab S2. Details on all specimens included in this study.

see the file Tab_S2.xlsx

Tab S3. Robinson-Foulds distance matrix between the various phylogenetic inference methods.
The first row gives the alignment used for inference (L or H) and the second row the inference software used.

see file Tab_S3.xlsx

Tab S4. Ancestral state reconstruction using stochastic character mapping.

see file Tab_S4.xlsx

Tab S5. Scores and loadings from the phylogenetically corrected principal component analysis.

see file Tab_S5.xlsx

Tab S6. Results of PGLS analysis of states indicating reciprocal copulation versus hypodermic insemination on sperm length.
All predictors were binary, with the reference level being the state indicating hypodermic insemination.

see file Tab_S6.xlsx

Tab S7. Results from PGLS correlating the first principal components of a phylogenetically corrected principal component analysis (pPCA) analysis including five stylet traits with the first principal component of a pPCA analysis including four antrum traits.
Analysis was performed across all species and restricted to the reciprocal mating syndrome. Also given are pPCA loadings and results for all three phylogenies.

see file Tab_S7.xlsx

Tab S8. Details on the transcriptomes used in this study.

see file Tab_S8.xlsx

Tab S9. Mean species values for all morphological variables.

see file Tab_S9.xlsx